arXiv:2302.13425v5 [cs.LG] 15 Jul 2024

A Survey on Uncertainty Quantification Methods for Deep Learning

WENCHONG HE, The University of Florida, USA
ZHE JIANG*, The University of Florida, USA
TINGSONG XIAO, The University of Florida, USA
ZELIN XU, The University of Florida, USA
YUKUN LI, Tufts University, USA

Deep neural networks (DNNs) have achieved tremendous success in making accurate predictions for computer vision, natural language processing, as well as science and engineering domains. However, it is also well-recognized that DNNs sometimes make unexpected, incorrect, but overconfident predictions. This can cause serious consequences in high-stake applications, such as autonomous driving, medical diagnosis, and disaster response. Uncertainty quantification (UQ) aims to estimate the confidence of DNN predictions beyond prediction accuracy. In recent years, many UQ methods have been developed for DNNs. It is of great practical value to systematically categorize these UQ methods and compare their advantages and disadvantages. However, existing surveys mostly focus on categorizing UQ methodologies from a neural network architecture's perspective or a Bayesian perspective and ignore the source of uncertainty that each methodology can incorporate, making it difficult to select an appropriate UQ method in practice. To fill the gap, this paper presents a systematic taxonomy of UQ methods for DNNs based on the types of uncertainty sources (data uncertainty versus model uncertainty). We summarize the advantages and disadvantages of methods in each category. We show how our taxonomy of UQ methodologies can potentially help guide the choice of UQ method in different machine learning problems (e.g., active learning, robustness, and reinforcement learning). We also identify current research gaps and propose several future research directions.

CCS Concepts: • **Computing methodologies → Uncertainty quantification**; **Machine learning approaches**; **Knowledge representation and reasoning**; • **Applied computing → Physical sciences and engineering**; • **Information systems → Data mining**.

Additional Key Words and Phrases: Deep learning, uncertainty quantification, data uncertainty, model uncertainty, trustworthy AI.

ACM Reference Format:
Wenchong He, Zhe Jiang, Tingsong Xiao, Zelin Xu, and Yukun Li. 2023. A Survey on Uncertainty Quantification Methods for Deep Learning. *ACM Comput. Surv.* 37, 4, Article 111 (August 2023), 41 pages. https://doi.org/XXXXXXX.XXXXXXX

*Contact author

Authors' addresses: Wenchong He, whe2@ufl.edu, The University of Florida, Gainesville, FL, USA, 32611; Zhe Jiang, zhe.jiang@ufl.edu, The University of Florida, Gainesville, FL, USA, 32611; Tingsong Xiao, xiaotingsong@ufl.edu, The University of Florida, Gainesville, FL, USA, 32611; Zelin Xu, zelin.xu@ufl.edu, The University of Florida, Gainesville, FL, USA, 32611; Yukun Li, yukun.li@tufts.edu, Tufts University, Medford, MA, USA, 02155.

Permission to make digital or hard copies of all or part of this work for personal or classroom use is granted without fee provided that copies are not made or distributed for profit or commercial advantage and that copies bear this notice and the full citation on the first page. Copyrights for components of this work owned by others than ACM must be honored. Abstracting with credit is permitted. To copy otherwise, or republish, to post on servers or to redistribute to lists, requires prior specific permission and/or a fee. Request permissions from permissions@acm.org.
© 2023 Association for Computing Machinery.
0360-0300/2023/8-ART111 $15.00
https://doi.org/XXXXXXX.XXXXXXX

1 INTRODUCTION

Deep neural network (DNN) models have achieved remarkable success in computer vision, natural language processing, as well as science and engineering domains [37, 91, 134]. Existing popular DNN models can be largely regarded as a deterministic function, which maps the input features to a target prediction through hierarchical representation learning [12]. While these DNN models often achieve strong performance in overall prediction accuracy, it is also well-recognized that they sometimes make unexpected, incorrect, but overconfident predictions, especially in a complex real-world environment [143]. This can cause serious consequences in high-stake applications, such as autonomous driving [30], medical diagnosis [10], and disaster response [4].

In this regard, a DNN model should be aware of what it does not know in order to avoid overconfident predictions. For example, in the medical domain, when DNN-based automatic diagnosis systems encounter uncertain cases, a patient should be referred to a medical expert for more in-depth analysis to avoid fatal mistakes. In an autonomous vehicle, if a DNN model knows in what scenarios (e.g., bad weather) it tends to make mistakes in estimating road conditions, it can warn the driver to take over and avoid potential crashes.

"Knowing what a DNN model does not know" comes down to placing appropriate uncertainty scores in its predictions, also called uncertainty quantification (UQ). Uncertainty in DNNs may come from different types of sources, including data uncertainty and model uncertainty [186]. Data uncertainty (also aleatory uncertainty) is an inherent property of the data, which originates from the randomness and stochasticity of the data (e.g., sensor noises) or conflicting evidence between the training labels (e.g., class overlap). Data uncertainty is often considered irreducible because we cannot reduce it by adding more training samples. Model uncertainty (also epistemic uncertainty), on the other hand, comes from the lack of evidence or knowledge during model training or prediction for a new test sample, e.g., limited training samples, sub-optimal DNN model architecture or parameter learning, and out-of-distribution (OOD) samples.

In recent years, researchers have developed a growing number of UQ methods for DNN models. However, as shown in Fig. 1, existing surveys of UQ methods for DNNs are either from a neural network architecture's perspective or a Bayesian perspective, ignoring the type of uncertainty sources. Specifically, [52] categorizes existing UQ methods based on their types of DNN model architectures, including Bayesian neural networks, ensemble models, and single model architecture, but it does not discuss the connection between the DNN model architectures and the type of uncertainty sources they incorporate. Other surveys only focus on the Bayesian perspective. For example, [115] gives a comprehensive review of Bayesian neural networks for UQ but ignores existing methods from the frequentist perspective (e.g., prediction interval, ensemble methods). [1] covers the ensemble and other frequentist methods, but it does not compare their advantages and disadvantages. To the best of our knowledge, existing surveys on UQ methods often ignore the types of uncertainty sources they incorporate. This perspective is important for selecting the appropriate UQ methods for different applications, where one type of uncertainty dominates others.

To fill the gap, we provide the first survey of UQ methods for DNNs from an uncertainty source's perspective. Specifically, we create a systematic taxonomy for DNN uncertainty quantification methodologies based on the type of uncertainty sources that they incorporate. We summarize the characteristics of different methods in their technical approaches and compare the advantages and disadvantages when addressing different types of uncertainty sources. We also connect the taxonomy to several major deep learning topics where UQ methods are critical, including OOD detection, active learning, and deep reinforcement learning. Lastly, we identify the research gaps and point out several future research directions.

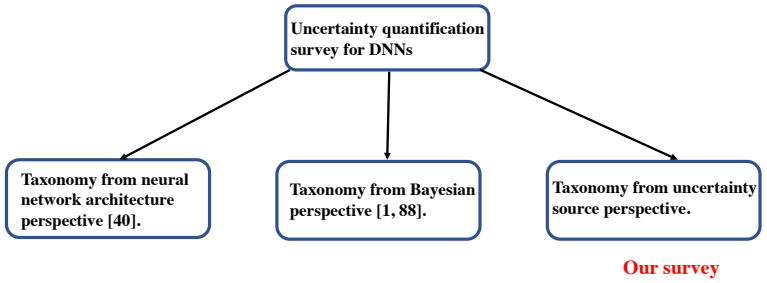

Fig. 1. Existing survey on UQ for DNN models

2 SUPERVISED LEARNING PROBLEM DEFINITION

Given training data $\mathcal{D}_{tr} = \{\boldsymbol{x}_i, y_i\}_{i=1}^n \subset \mathcal{X} \times \mathcal{Y}$, $\mathcal{X}$ is the input sample space, and $\mathcal{Y}$ is the target variable space for the input sample. Each training instance is assumed to be independent and identically distributed (i.i.d.) from some unknown probability distribution $p(\boldsymbol{x}, y)$ on the space $\mathcal{X} \times \mathcal{Y}$. Given a hypothesis space $\mathcal{H}$ consisting of hypotheses $h : \mathcal{X} \to \mathcal{Y}$ and a loss function l that measures the discrepancy between prediction and ground-truth, a learning problem aims to find the best hypothesis in the hypothesis space that minimizes the loss [13, 69]:

$$h^* = \arg\min_{h \in \mathcal{H}} R(h), \quad \text{where} \quad R(h) = \int l(y, h(\boldsymbol{x}))p(\boldsymbol{x}, y)d\boldsymbol{x}dy \tag{1}$$

In practice, the model is fitted by minimizing the empirical risk [120], defined as the average loss over the training data $\mathcal{D}_{tr}$:

$$\tilde{h} = \arg\min_{h \in \mathcal{H}} R_{emp}(\mathcal{D}_{tr}, h), \text{ where } R_{emp}(\mathcal{D}_{tr}, h) = \frac{1}{n}\sum_{i=1}^{n} l(y_i, h(\boldsymbol{x}_i)) \tag{2}$$

3 TYPES OF UNCERTAINTY SOURCE

Based on the mathematical formulation of supervised learning in Section 2, we provide the definitions for two major types of uncertainty, data uncertainty and model uncertainty. We discuss the sources of each type and their representations.

3.1 Model uncertainty

3.1.1 Source of model uncertainty. The model uncertainty (aka epistemic uncertainty) represents the uncertainty in the model's predictions related to the imperfect model training process (e.g., due to a lack of knowledge of model choices based on the current input data). It is reducible given more training data. There are several common types of model uncertainty: uncertainty in model architecture; uncertainty in the model parameters; and uncertainty due to different sample distribution selections. Different kinds of uncertainty sources are shown in Fig. 2, where $\mathcal{F}$ denotes the entire hypothesis space of different neural network architectures and parameters, $\mathcal{H}$ is the hypothesis space for one particular model architecture. h^* is the optimal solution in $\mathcal{H}$

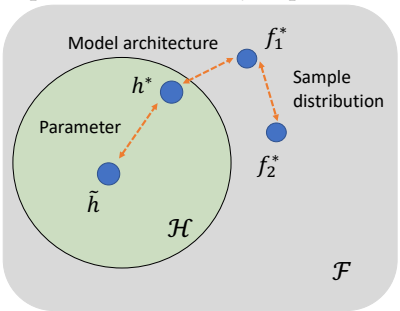

Fig. 2. Visualization on various model uncertainty sources.

assuming a specific model architecture. $\hat{h}$ is the optimal solution in $\mathcal{H}$ with the empirical loss based on training data $\mathcal{D}_{tr}$ (see Eq. 2). f_1^* and f_2^* are the theoretical optimal hypotheses for two different sample distributions $p_1(\boldsymbol{x}, y)$ and $p_2(\boldsymbol{x}, y)$ based on Eq. 1, that is $f_i = \arg\min_{h \in \mathcal{F}} \int l(y, h(\boldsymbol{x})) p_i(\boldsymbol{x}, y) d\boldsymbol{x} dy$ for $i = 1, 2$.

Table 1 summarizes different sources of model uncertainty in the supervised learning framework. The first type, model architecture uncertainty is due to the lack of knowledge of which type of model architecture is most suitable for the data. Because of this, the optimal solution h^* selected from $\mathcal{H}$ under specific architecture (hypothesis space) is different from the theoretical optimal f^*. This is true even if the learning algorithm is perfect. Second, due to limited training data or imperfect learning algorithms in the optimization process, the learned optimal solution $\hat{h}$ with the empirical training loss may not align to the optimal solution h^* with the specific architecture $\mathcal{H}$. This leads to model uncertainty related to model parameter learning. Third, model uncertainty can be related to the (training) sample distribution. For instance, learning samples may come from different distributions, e.g., $p_1(\boldsymbol{x}, y)$ and $p_2(\boldsymbol{x}, y)$. Thus, the theoretical optimal solution f^* varies for different population distributions, causing uncertainty in model predictions on out-of-distribution samples. In addition, when a model makes predictions on a test sample that is far away from other training samples (or surrounded by sparse training samples) in the feature space $\mathcal{X}$ (see Fig. 7), the prediction tends to have higher uncertainty. Note that the three types of model uncertainty sometimes overlap with each other. Model uncertainty related to sample distribution is also connected to uncertainty in parameter learning. For example, model uncertainty due to the lack of training samples near a test sample can also be considered as model parameter learning uncertainty.

Table 1. The corresponding supervised learning notation for different model uncertainty sources

Model uncertainty source	**Corresponding notation in supervised learning framework**
Model architecture	Optimal solution h^* in $\mathcal{H}$ does not align with theoretical optimal f^* in $\mathcal{F}$
Model parameters	Learned model $\tilde{h}$ does not align with optimal $h*$ in $\mathcal{H}$
Sample distribution	Theoretical optimum f_1^* and f_2^* mismatch under different sample distribution $p(\boldsymbol{x}, y)$

3.1.2 Model uncertainty representation. As discussed above, the source of model uncertainty can arise from three different aspects: model parameters, model architectures, and the sample distribution. In general, different methods are adopted to represent the model uncertainty from each type. First, uncertainty from model parameters is from the lack of knowledge of optimal parameters for the given problem. It can be estimated with a Bayesian neural network (BNN) [77]. BNN assumes a prior over the model parameters and aims to infer the posterior distribution of model parameters to reflect the parameter uncertainty. Second, uncertainty arising from the model architectures is due to the lack of knowledge regarding the optimal hypothesis space. It can be estimated with ensembles of neural networks (deep ensembles). The intuition is to construct an ensemble of neural network architectures and each model is trained separately. The predictions of the ensemble on an input form a distribution on the target variable. Thus the variance of the target variable predictions can be an estimation of the prediction uncertainty. The third type is the uncertainty from sample distribution, which is caused by the mismatch between the training dataset distribution and that of the test samples. More details of the categorization and methods are discussed in Section 5.

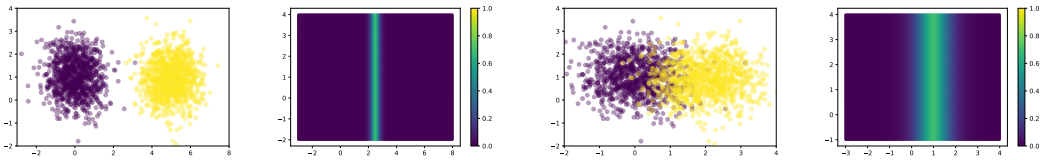

(a) Classes distribution with clean separable boundary (b) Entropy of samples in (a) (c) Classes distribution with ambiguous boundary (d) Entropy of samples in (c)

Fig. 3. Data uncertainty visualization examples (Different colors represent samples in different classes)

3.2 Data uncertainty

3.2.1 Source of data uncertainty. Data uncertainty (aka aleatoric uncertainty) arises from the data's inherent randomness, noise, or overlapping feature distribution in different classes, which is irreducible even with more training data [186]. Randomness or noise in data can arise in data acquisition. The uncertainty in the data acquisition process is due to instrument errors, inappropriate frequency of data acquisition, and data transmission errors [60]. For example, certain data acquisition devices cannot work properly in a complex environment (e.g., poor weather conditions). Inappropriate sampling methods, data storage, data representation methods, and interpolation techniques also affect uncertainty during data processing [186].

For example, for spatiotemporal data collected from various space and airborne platforms (e.g., CubeSat, UAVs), the data uncertainty may result not only from the sensor errors associated with the data acquisition devices but also from the fact that data are acquired in a digital format (which is discrete in nature) [29] even though the underlying phenomenon is continuous. The uncertainty of the representation of an object's movement is also affected by the frequency with which location samples are taken, i.e., the sample rate [137]. Uncertainty in the data can also accumulate from multiple sources and may be propagated into the model.

3.2.2 Data uncertainty representation. Consider a training dataset $\mathcal{D}_{tr}$ drawn from the distribution $p(\boldsymbol{x}, y)$ over the d dimension input features $\boldsymbol{x} \in \mathbb{R}^d$ and target class labels $y \in \{\omega_1, ..., \omega_k\}$ for a classification problem with k classes or $y \in \mathbb{R}$ for a regression model. There are several techniques for data uncertainty representation to account for the inherent randomness between the mapping from $\boldsymbol{x}$ to y. In the context of a discriminative classification task, one method to represent the uncertainty of the class variable given a specific input $\boldsymbol{x}$ is the maximum class probability $\max p(y|\boldsymbol{x})$. Another method uses the entropy of the condition class distribution $p(y|\boldsymbol{x})$, which describes the randomness of the class distribution due to the overlap of feature values among samples in different classes. One other method is set-based methods, e.g., conformal prediction [154], which aims to ensure the correct answer in the prediction set with a predefined confidence level.

Data uncertainty arises from the data's natural complexity and the class boundary structure on the feature space. Take a toy distribution in Fig. 3 as an example, which consists of two normally distributed clusters. Each cluster (color) represents a separate class. The dataset in Fig. 3 (a) has a clearer class boundary (lower data uncertainty). The entropy of most samples is low except for those near the class boundary, as in Fig. 3 (b). In contrast, the dataset in Fig. 3 (c) has more overlap between the two classes, corresponding to higher data uncertainty in Fig. 3 (d).

Beyond the inherent complex class boundary, data uncertainty can also come from the inherent noise (variability) in the data generation or collection process. For example, for a regression problem, the observations can be represented by: $y = f(\boldsymbol{x}) + \epsilon(\boldsymbol{x})$, where $f(\boldsymbol{x})$ is the true data generation

function, and $\epsilon(\boldsymbol{x})$ represents the measurement noise in the dataset. There are two classes of noise: homoscedastic and heteroscedastic noise [82]. Homoscedastic noise assumes a constant observation noise over all the inputs $\boldsymbol{x}$. Heteroscedastic noise, on the other hand, models the observation noise as a function of input $\epsilon(\boldsymbol{x}) \sim p(\epsilon|\boldsymbol{x})$ (e.g., heteroscedastic Gaussian noise). The heteroscedastic noise model is useful in the case where the noise level varies for different samples.

3.3 Summary

In summary, we highlight two primary types of uncertainty and discuss their potential sources and representations. As Fig. 4 shows, data uncertainty arises from the inherent property of the input data features and labels, and model uncertainty stems from the misspecification of model architectures, parameters, and the dataset distribution shift. Depending on the nature of the application, the predominant type of uncertainty may vary, and specific methods may be necessary to address them. These uncertainties underscore the importance of robust analysis and interpretation of data and model outputs in various fields.

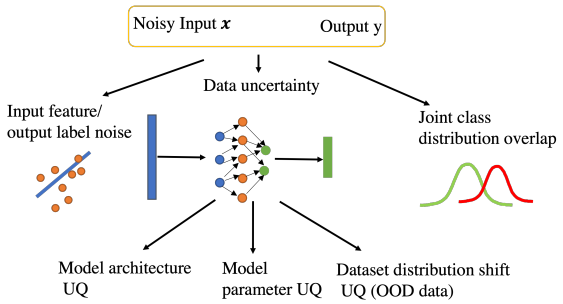

Fig. 4. Different types of uncertainty source

4 APPLICATION DOMAINS

In this section, we discuss several application domains of uncertainty quantification for deep learning models. For each application domain, we discuss the motivation for developing uncertainty-aware models and the nature of the data, the source of uncertainty, and the challenges associated with uncertainty quantification.

Medical diagnosis: Deep neural network models have achieved tremendous success in a wide variety of medical applications, including medical imaging, clinical diagnosis support, and treatment planning [21, 31, 131, 171]. However, one critical concern is that deep learning models tend to be over-confident even for a wrong prediction [105], causing serious consequences. Thus, we need to estimate the prediction uncertainty (confidence). Both data uncertainty and model uncertainty exist in medical problems. Data uncertainty comes from noisy measurements from medical devices, ambiguous class labels (e.g., non-consensus tumor boundary annotations on imagery between different radiologists), and registration errors between medical imagery taken at different times or from different devices [55]. Model uncertainty also exists because patient subjects in the test cases may not be well-represented in the training set. There exist several challenges to developing UQ methods. First, there is diverse noise or uncertainty in medical data. Second, interpretability in uncertainty quantification is important, which is not well solved in medical problems. Existing uncertainty-aware deep learning models in medical domains can be categorized into those related to medical imaging and those for non-medical imaging applications [105]. In medical imaging,

deep learning is often used for segmentation or classification for MRI, ultrasound, and coherence tomography (CT) imagery [45, 85]. These studies often focus on data uncertainty due to ambiguous labels [123, 141], or image registration uncertainty [27]. Non-medical imaging applications are mostly related to clinical diagnosis support and treatment planning from Electronic Health Records (EHR). Recurrent neural networks and graph neural networks have been applied to EHR data to predict patient diseases and possible treatment [191]. The presence of significant variability in personalized predictions [44] requires a model to capture prediction uncertainty.

Geoscience: With the advance of GPS and remote sensing technologies, a growing volume of spatiotemporal data is collected from spaceborne, airborne, seaborne, and terrestrial platforms [48, 122, 155]. The emerging spatiotemporal big data, increasing computational power (GPUs), and the recent advances in deep learning technologies provide unique opportunities for advancing our knowledge about the Earth system [143]. For example, deep learning has been used to predict river flow and temperature [70] and hurricane tracks [83]. Uncertainty quantification for deep learning is important in geoscience because of the high-stakes decision-making involved (e.g., evacuation planning based on hurricane tracking with a "cone of uncertainty"). Several challenges exist due to the unique characteristics of spatiotemporal data. First, spatiotemporal data have various spatial, temporal, and spectral resolutions and diverse sources of noise and errors (e.g., sensor noise, obstacles, and atmospheric effects in remote sensing signals [98], GPS errors). Second, spatial registration error and uncertainty may exist when co-registering different layers of geospatial data into the same spatial reference system [61]. Third, spatiotemporal data are heterogeneous, i.e., the data distribution often varies across different regions or time periods [74]. Thus, a deep learning model trained in one region (or time) may not generalize well to another region (or time). This issue is particularly important when spatial observation samples are sparsely distributed, causing uncertainty when inferring the observations at other locations in continuous space [38, 39, 65].

Transportation: Deep learning for transportation data (e.g., ground sensors and video cameras on the road) provides unique opportunities to monitor traffic conditions, analyze traffic patterns, and improve decision-making. For instance, temporal graph neural networks are used to predict traffic flows(e.g., congestion or accidents) [104, 118, 192]. Deep learning plays a critical role in autonomous driving (e.g., using lidar sensors and optical cameras to detect road lanes and other vehicles or pedestrians). Uncertainty quantification for AI in transportation is challenging due to the temporal dynamics, complex road environment, and the existence of noise and uncertainty (e.g., omission, sparse sensor coverage, errors, or inherent bias). For example, highly crowded events can disrupt normal traffic flows on road networks. Existing works on trajectory prediction uncertainty consider the data uncertainty due to the sparse or insufficient training data [194], and erroneous or missing measurements due to signal loss [113]. Other works consider complex environmental factors such as extreme weather [94, 135, 176, 195]. Uncertainty in short-term traffic status forecasting (such as volume, travel speeds, and occupancy) is related to the stochastic environment and model training [175], while uncertainty in long-term traffic modeling comes from the exogenous factors of traffic flow (e.g., rainstorms and snowstorms) [96].

Biochemistry engineering: Traditional biochemistry discoveries are primarily based on experiments, which are expensive and time-consuming [17]. With the rapid advancement of computational science, researchers have turned to simulation and data-driven approaches to aid scientific discovery [20]. Simulation methods create mathematical models based on fundamental principles, such as kinetics of microbial growth and product synthesis, fluid dynamics in bioreactors, and design of new proteins and enzymes [119]. However, these models can be computationally intensive and require an in-depth understanding of the biochemical system. In contrast, deep learning-based models use neural networks and a vast amount of biochemistry data to directly extract knowledge and learn complex relationships. However, the common data-driven DNN models are unaware of domain

knowledge and face challenges in representing the complexities of biochemical systems, such as the heterogeneity of microbial populations and genetic-environmental variations. This often results in unreliable outputs that require human experts to verify, adding additional labor to the process [66]. In the realm of drug discovery, although AlphaFold has achieved remarkable success in predicting protein structures—an essential factor in determining protein properties—there remains considerable uncertainty in these predictions. This is because deep learning models lack first-principle biochemical knowledge that would govern such predictions. Thus, Uncertainty-aware deep learning models are crucial as calibrated uncertainty provides information on what they do not know and can potentially help identify novel chemical structures and chemical species whose data may be associated with significant noise [184].

Several factors contribute to the uncertainty of data-driven biochemistry engineering. For example, researchers often have only a partial understanding of the complex biological mechanism and the macro-molecules released from the cells and it is difficult to quantify the heterogeneity in the microbial population, due to genetic and environmental variations. For different tasks, these factors may play a different role in the UQ for the neural network model. In protein engineering, the protein function prediction (based on protein sequences, protein structures, and protein-protein interactions) is challenging because of the large amount of diversity of protein folds and the lack of a complete understanding of the protein structure [18]. For bioreactor engineering, the prediction of bioreactor system performance is affected by the intrinsic interactions between bioreactor operating factors (e.g., pH, temperature, and substrate concentration). An iterative method has been used to enable the propagation of model uncertainty for multi-step ahead predictions [119].

Natural Language Processing: The advancement of pre-trained language models (PLMs) has revolutionized language processing by addressing various tasks in a unified manner [95]. Although natural language processing (NLP) has made remarkable strides with the emergence of large language models (LLMs), these models are prone to hallucination, often generating misleading or fabricated content [111, 183]. Thus, uncertainty quantification plays a critical role in improving the trustworthiness of LLMs in several applications, such as assessing the reliability of machine translations, gauging sentiment polarity in sentiment analysis, especially in ambiguous cases, and improving the accuracy and reliability of speech-to-text models in speech recognition. However, quantifying uncertainty in LLMs presents significant challenges. First, uncertainty can arise from various sources related to both data and model perspectives. Data uncertainty stems from ambiguities, noise (such as out-of-vocabulary words or distractions), and semantic complexities in the input language. Model uncertainty occurs when the model lacks the specific knowledge required for out-of-distribution input queries, leading to arbitrary responses, a phenomenon known as the hallucination problem in LLMs. Second, the large vocabulary space complicates the direct assessment of confidence through probability likelihood, and relying solely on prediction logits can lead to overconfidence [59]. Moreover, capturing uncertainty in the semantic space is essential due to the semantic similarity among different answers. Third, aligning uncertainty with actual correctness (calibration) is crucial for trustworthy applications of large language models.

Engineering Design: Engineering simulation accelerates the development of reliable and repeatable design processes. However, the computing resource consumption is dramatically raised in the whole development process. Deep learning-based methods have great potential to accelerate modern industrial product design in several aspects. First, the deep learning-based surrogate model for the physics process has the potential to accelerate the traditional simulation-based engineering process, for example, in material modeling [100], flow sculpting [93], distributed energy resources optimization [129]. Second, deep generative models have been successfully utilized for synthesis. For example, generative adversarial networks are leveraged to synthesize hierarchical designs with inter-part dependencies [26], intelligent computer-aided design (CAD) [26], 2D wheel design

[130]. Third, leveraging deep learning models can extract human preferences and design strategies from a large number of observation data [162]. However, in these applications, a major concern for deep learning in engineering design is the lack of trustworthiness in real-world applications. Through explicit uncertainty quantification, the model is aware of the potential mistakes it can make and facilitates broader adoption of deep learning in high-stakes decision-making, including manufacturing, aviation, and automotive engineering. The uncertainty source comes from diverse aspects, including data uncertainty due to measurement noise and randomness in the physics variable. Second is model uncertainty due to limited data availability in the engineering domain.

5 A TAXONOMY OF DNN UQ METHODOLOGY

In this section, we provide a new taxonomy of existing DNN UQ methods based on the type of uncertainty sources each method can capture. As mentioned before, two main sources of uncertainty exist in the DNN predictions, and for different domain applications, different sources may play a major role in affecting the model prediction. Thus it is vital to understand which type of uncertainty source each method can address. In general, we categorize existing works into three branches based on the uncertainty sources as Fig. 5 shows: model uncertainty, data uncertainty, and the combination of the two. We briefly introduce each category as follows:

- Model uncertainty: In this category, the approaches consider the model uncertainty resulting from the parameters (BNN), architectures (ensemble methods), or sample distribution (deep Gaussian process and distance-aware model).
- Data uncertainty: The approaches in this category aim to account for the uncertainty from the inherent randomness or noise in the data. The general idea is to construct a distribution over the prediction. These approaches are further split into deep discriminative models and deep generative models.
- The combination of model and data uncertainty: Many approaches aim to capture the total uncertainty in one framework, which is the combination of model and data uncertainty. The straightforward approach combines the approaches in data and model uncertainty, forming a coherent framework but introducing more computation and storage demand. Another framework called evidential deep learning overcomes the computational challenge with a single neural network model.

In the following, the main intuitions and approaches of the three types are presented and their main advantages and disadvantages are discussed.

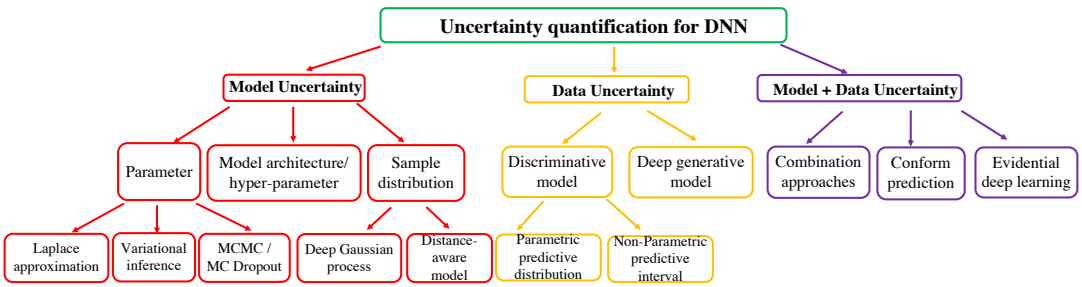

Fig. 5. A taxonomy for existing literature on UQ for DNN

5.1 Model Uncertainty

This subsection reviews the existing framework for DNN model uncertainty. We categorize the approaches into three subcategories: Bayesian neural network, ensemble models, and sample distribution-related models. We will introduce each subcategory in detail.

5.1.1 Bayesian Neural Networks. From a frequentist point of view, there exists a single set of parameters $\boldsymbol{\theta}*$ that fit the DNN model best, where $\boldsymbol{\theta}* = \arg\min_{\boldsymbol{\theta}} \mathcal{L}(\mathbf{Y}, f(\mathbf{X}, \boldsymbol{\theta}))$ and $\mathcal{L}$ is the loss function. However, the point estimation of DNN parameters tends to be over-fitting and overconfident [165]. In contrast, the Bayesian neural network (BNN) imposes a prior on the neural network parameters $p(\boldsymbol{\theta})$ and learns the posterior distribution of these parameters $p(\boldsymbol{\theta}|\mathbf{X}, \mathbf{Y})$.

$$p(\boldsymbol{\theta}|\mathbf{X}, \mathbf{Y}) = \frac{p(\mathbf{Y}|\mathbf{X}, \boldsymbol{\theta})p(\boldsymbol{\theta})}{p(\mathbf{Y}|\mathbf{X})} \tag{3}$$

This term is the posterior distribution of model parameters conditioned on the training dataset. This distribution reflects what extent our model can capture the training data pattern. Assuming a Gaussian distribution for the model parameters, the larger the variance of the distribution is, the larger uncertainty there exists in the model. Such uncertainty can be caused by a small amount of training data or inappropriate configuration of neural network architecture.

For inference on the new samples $\boldsymbol{x}*$, we can marginalize out the model parameters by:

$$p(y* | x*, \mathbf{X}, \mathbf{Y}) = \int p(y* | \boldsymbol{x}*, \boldsymbol{\theta}) p(\boldsymbol{\theta}|\mathbf{X}, \mathbf{Y}) d\boldsymbol{\theta} \tag{4}$$

The uncertainty on the test samples will be reflected by the prediction distribution variance.

However, the approach is analytically intractable and does not have a closed-form solution and an approximation must be made for prediction in BNN. To estimate the posterior of the neural network parameters, various approaches have been proposed to approximate the parameter posterior in a simpler form to solve it in a tractable way. Some approximation methods define **a parameterized class of distributions,** $\boldsymbol{Q}$, from which they select an approximation $q_\phi(\boldsymbol{\theta})$for the posterior. For example, $\boldsymbol{Q}$ can be the set of all factorized Gaussian distributions, and ϕ is the parameters of mean and diagonal variance. The distribution $q_\phi(\boldsymbol{\theta}) \in \boldsymbol{Q}$ is selected according to some optimization criteria to approximate the posterior. Two popular approaches for optimization are *variational inference* [16] and *Laplace approximation* [49]. Instead of approximating the posterior analytically, another approach aims to solve this problem by Monte Carlo sampling called *Markov Chain Monte Carlo sampling*. In the following, we will review existing methodologies in the three subcategories in detail.

Variational Inference (VI): In [57, 67], the authors propose to find a variational approximation to the Bayesian posterior distribution on the weights by maximizing the *evidence lower bound* (ELBO) of the log marginal likelihood. The intractable posterior $p(\boldsymbol{\theta}|\mathbf{X}, \mathbf{Y})$ is approximated with a parametric distribution $q_{\boldsymbol{\phi}}(\boldsymbol{\theta})$.

$$\log p(\mathbf{Y}|\mathbf{X}) \geq \mathbb{E}_{\boldsymbol{\theta}\sim q_\phi(\boldsymbol{\theta})} \log \frac{p(\mathbf{Y}|\mathbf{X}, \boldsymbol{\theta})p(\boldsymbol{\theta})}{q_\phi(\boldsymbol{\theta})} = \mathbb{E}_{\boldsymbol{\theta}\sim q_\phi(\boldsymbol{\theta})} \log p(\mathbf{Y}|\mathbf{X}, \boldsymbol{\theta}) - \mathcal{KL}(q_\phi(\boldsymbol{\theta})||p(\boldsymbol{\theta})) \tag{5}$$

where the first term $\mathbb{E}_{\boldsymbol{\theta}\sim q_\phi(\boldsymbol{\theta})} \log p(\mathbf{Y}|\mathbf{X}, \boldsymbol{\theta}))$ is log-likelihood of the training data on the neural network model. This term increases as the model accuracy increases. The second term is the *Kullback-Leibler* (KL) divergence between the posterior estimation and the prior of the model parameters, which controls the complexity of the neural network model. Maximizing Eq. 5 corresponds to finding a tradeoff between the prediction accuracy and complexity of the model. Thus the posterior inference problem becomes an optimization problem on the parameter $\boldsymbol{\phi}$.

One challenge of variational inference lies in the choice of the parameterized class of distribution $q_{\boldsymbol{\phi}}(\boldsymbol{\theta})$. The original method relies on the use of Gaussian approximating distribution with

a *diagonal* covariance matrix (mean-field variational inference) [67, 139]. This method leads to a straightforward lower bound for optimization, but the approximation capability is limiting. To capture the posterior correlations between parameters, the second category of approaches extends the diagonal covariance to *general* covariance matrix while still leading to a tractable algorithm by maximizing the above ELBO [138]. However, the full covariance matrix not only increases the number of trainable parameters but also introduces substantial memory and computational cost for DNN. To reduce the computation, the third category of approaches aims to simplify the covariance matrix structure with certain assumptions. Some approaches assume independence among layers, resulting in *block-diagonal structure* covariance matrix [161, 189]. Others find that for a variety of deep BNN trained using Gaussian variational inference, the posterior consistently exhibits strong low-rank structure after convergence [164], they propose to decompose the dense covariance matrix into a low-rank factorization to simplify the computation. Additionally, [117] assumes the covariance matrix taking the form of *"diagonal plus low-rank"* structure for a more flexible and faster approximation. Another line of work introduces sparse uncertainty structure via a hierarchical posterior or employing normalizing flow with low-dimensional auxiliary variables [106, 148] to reduce the computation.

The disadvantage of variational Gaussian approximation for DNN parameters is that to capture the full correlations among model latent weights, it requires a large number of variational parameters to be optimized, which scales quadratically with the number of latent weights in the model. Existing works aim to simplify the covariance structure with certain assumptions while still capturing the correlation between neural network parameters to optimize the computational speed.

Laplace approximation: The idea behind the Laplace approximation is to obtain an approximate posterior around the *'maximum a posterior'* (MAP) estimator of neural network weights with a Gaussian distribution, based on the second derivative of the neural network likelihood functions [108]. The method can be applied post hoc to a pre-trained neural network model.

$$p(\boldsymbol{\theta}|\mathbf{X},\mathbf{Y}) \approx p(\hat{\boldsymbol{\theta}}|\mathbf{X},\mathbf{Y}) \exp(-\frac{1}{2}(\boldsymbol{\theta}-\hat{\boldsymbol{\theta}})^T \mathbf{H} (\boldsymbol{\theta}-\hat{\boldsymbol{\theta}})) \tag{6}$$

Thus, the posterior is then approximated as a Gaussian:

$$p(\boldsymbol{\theta}|\mathbf{X},\mathbf{Y}) = \mathcal{N}(\hat{\boldsymbol{\theta}}, \mathbf{H}^{-1}) \tag{7}$$

Where $\hat{\boldsymbol{\theta}}$ is the MAP estimate and $\mathbf{H}$ is the Hessian matrix. It is the second derivative of the neural network likelihood function regarding the model weights, i.e., $\mathbf{H}_{ij} = -\frac{\partial^2}{\partial\boldsymbol{\theta}_i \partial\boldsymbol{\theta}_j} \log p(\mathbf{Y}|\mathbf{X},\boldsymbol{\theta})$. Fig. 6 (a) illustrates the intuition of Laplace approximation, where the blue density function is the true posterior distribution and the orange Gaussian distribution is the Laplace approximation. This method approximates the posterior locally and can simplify the computation of the posterior, but the downside is that it cannot capture the multi-modal distribution with more than one mode since it is a local estimation around the MAP mode.

Moreover, for DNN, it is still infeasible to compute the inverted Hessian matrix for all parameters, which is typically in the order of several million. Previous work on using Laplace approximation for neural network uncertainty quantification mainly aims to leverage the techniques of Hessian approximation to simplify the computation. One simple solution is to ignore the covariance between weights and only extract the diagonal of the Hessian matrix. Such methods Inspired by the *Kronecker factored approximations* of the curvature of a neural network, the approach [147] factorizes the Hessian matrix into the Kronecker product (matrix operation that results in a block matrix) of two smaller matrices. The method brings down the inversion cost of the Hessian matrix and can be scaled to deep convolutional networks and applied to Bayesian online learning efficiently [146]. However, the method introduces an additional assumption that each layer of the neural network is

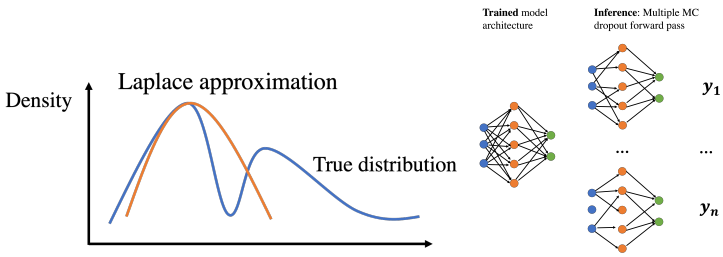

Fig. 6. Illustration of model uncertainty methods

independent (ignoring covariance between layers), which might lead to an overestimation of the variance (uncertainty) in certain directions.

To make the Laplace approximation allow for uncertainty quantification for contemporary DNN, another challenge is to calibrate the predictive uncertainty. One standard practice is to tune the prior precision of the Gaussian prior on model weights [147]. This has a regularizing effect both on the approximation to the true Hessian, as well as the Laplace approximation itself, which may be placing probability mass in low probability areas of the true posterior. However, these parameters require optimization w.r.t. the prediction uncertainty performance on a validation dataset, which may not generalize well on new test data. To overcome this disadvantage, another approach introduces a more flexible framework to tune the uncertainty of Laplace-approximated BNNs by adding some additional '*hidden units*' to the hidden layer of MLP-trained network [88]. The framework is trained with an uncertainty-aware objective to improve the uncertainty calibration of Laplace approximations. However, the limitation of this method is it can only be applied to MLP-trained networks, and cannot generalize to other models, e.g., convolutional neural networks.

To sum up, the previous methods employed optimization-based schemes like variational inference and Laplace approximations of the posterior. In doing so, strong assumptions and restrictions on the form of the posterior are enforced. The common practice is to approximate the posterior with a Gaussian distribution. The restrictions placed are often credited with inaccuracies induced in predictions and uncertainty quantification performance. The difference between the two approximations is that the Laplace approximation is a local approximation around the MAP estimation, and it can be applied to a pre-trained neural network and obtain uncertainty quantification without influencing the performance of the neural network. On the other hand, the variational inference is a global optimization used during training and may influence the model prediction performance.

Markov Chain Monte Carlo approximation: Markov Chain Monte Carlo (MCMC) is a general method for sampling from an intractable distribution. MCMC constructs an ergodic Markov chain whose stationary distribution is posterior $p(\boldsymbol{\theta}|\mathbf{X}, \mathbf{Y})$. Then we can sample from the stationary distribution. The inference step of BNN (Eq. 4) can be approximated as the following equation:

$$p(y*|x*, \mathbf{X}, \mathbf{Y}) = \int p(y*|\boldsymbol{x}*, \boldsymbol{\theta}) p(\boldsymbol{\theta}|\mathbf{X}, \mathbf{Y}) d\boldsymbol{\theta} \approx \frac{1}{N} \sum_{i=1}^{N} p(y*|x*, \boldsymbol{\theta}_i) \tag{8}$$

where $\boldsymbol{\theta}_i \sim p(\boldsymbol{\theta}|\mathbf{X}, \mathbf{Y})$ is a sampled from MCMC. This process generates samples by a Markov chain over a state space, where each sample only depends on the state of the previous sample. The dependency is described with a proposal distribution $T(\boldsymbol{\theta}'|\boldsymbol{\theta})$ that specifies the probability density of transitioning to a new sample $\boldsymbol{\theta}'$ from a given sample $\boldsymbol{\theta}$. Some acceptance criteria are based on

the relative density (energy) of two successive samples evaluated at the posterior to determine whether to accept the new sample or the previous sample. The vanilla implementation is through the *Metropolis-Hastings* algorithm [120] with Gaussian proposal distribution $T(\boldsymbol{\theta}'|\boldsymbol{\theta}) \sim \mathcal{N}(\boldsymbol{\theta}, \Sigma)$. Specifically, in each iteration, the algorithm constructs a Markov chain over the state space of $\boldsymbol{\theta}$ with the proposal density distribution. The proposal samples is stochastically accepted with the acceptance probability $\alpha(\boldsymbol{\theta}', \boldsymbol{\theta}) = \frac{T(\boldsymbol{\theta}'|\boldsymbol{\theta})p(\boldsymbol{\theta}'|x)}{T(\boldsymbol{\theta}|\boldsymbol{\theta}')p(\boldsymbol{\theta}|\boldsymbol{x})}$ via a random variable μ drawn uniformly from the interval $[0, 1]$ ($\mu \sim \text{Unif}(0, 1)$). If we reject the proposal sample, we retain the previous sample $\boldsymbol{\theta}$. This strategy ensures the stationary distribution of the samples converges to the true posterior after a sufficient number of iterations. However, the isotropic Gaussian proposal distribution shows random walk behavior and can cause slow exploration of the sample space and a high rejection rate. Thus it takes a longer time to converge to the stationary distribution. The problem is more severe because of the high dimensional parameter space of modern DNN which hinders the application of MCMC on neural network parameter sampling [124].

The recent development on MCMC for modern DNN mainly focuses on how to sample more efficiently and reduce convergence iterations. For example, One direction aims to combine the MCMC sampling with variational inference [151, 181] to take advantage of both methods. Since variational inference approximates the posterior by formulating an optimization problem w.r.t. the variational posterior is selected from a fixed family of distributions. This approach could be fast by ensuring some constraints on the variational posterior format, but they may approximate the true posterior poorly even with very low ELBO loss. On the other hand, MCMC does not have any constraints on the approximated posterior shape, and can potentially approximate the exact posterior arbitrarily well with a sufficient number of iterations. *Markov Chain Variational Inference* (MCVI) bridge the accuracy and speed gap between MCMC and VI by interpreting the iterative Markov chain $q(\boldsymbol{\theta}|x) = q(\boldsymbol{\theta}_0) \prod_{t=1}^{T} q(\boldsymbol{\theta}_t|\boldsymbol{\theta}_{t-1}, x)$ as a variational approximation in the expanded space with $\boldsymbol{\theta}_0, ...\boldsymbol{\theta}_{T-1}$. Thus, instead of constructing a sequential Markov Chain to sample $\boldsymbol{\theta}_0, ...\boldsymbol{\theta}_{T-1}$, they use another auxiliary variational inference distribution $r(\boldsymbol{\theta}_0, ..., \boldsymbol{\theta}_{T-1})$ to approximate the true distribution with some flexible parametric form. By optimizing the lower bound over the parameters of the variational distribution with a neural network, we can obtain the samples.

The advantage of MCMC methods is that the samples it gives are guaranteed to converge to the exact posterior after a sufficient number of iterations. This property allows us the control the trade-off between sampling accuracy and computation. However, the downside of this method is that we do not know how many iterations are enough for convergence and it may take an excessive amount of time and computing resources.

Monte-Carlo (MC) dropout: MC dropout approach [50] is currently the most popular method for DNN uncertainty quantification in many domains due to its simplicity and ease of implementation. This approach demonstrates that the optimization of a neural network with a dropout layer can be equivalent to approximating a BNN with variational inference on the parametric Bernoulli distribution [50]. Uncertainty estimation can be obtained by computing the variance on multiple stochastic forward predictions with different dropout masks (switching off some neurons' activation) as Fig. 6 (b) shows. The average predictions with various weights dropout can be interpreted as doing the approximate integration over the model's weights (as Eq.4) whose variational distribution follows the Bernoulli distribution. The advantages of MC dropout are: First, it requires little modification to existing DNN architecture design, which allows for straightforward implementation in practice. Second, it mitigates the problem of representing uncertainty by sacrificing prediction accuracy since the methods only influence the inference step. However, though there is theoretical justification for the probabilistic interpretation of MC dropout from a variational approximation

perspective, in many uncertainty benchmark datasets, MC dropout tends to be less calibrated than other baseline UQ methods [59].

In summary, we summarize several types of approximation on BNN, which aim to reduce the computation and memory burden of BNN and make it scalable to modern deep neural networks. Those approximation methods can capture the model uncertainty associated with parameters to some extent. However, the drawback is that the process requires approximation, which may lead to inaccurate uncertainty estimation.

5.1.2 Ensemble models. Ensemble models combine multiple neural network models in the prediction process. The ensemble predictions form an output distribution. The prediction variability of the ensemble models can be a measure of model uncertainty (e.g., a larger variance implies larger uncertainty). To capture the model uncertainty arising from different aspects, several strategies for constructing ensembles can be adopted, summarized into three major categories: the first kind is through bootstrapping [90]. This is a strategy for random sampling from the original dataset with replacement. An ensemble of neural network models is constructed, each trained on different bootstrapped samples. After training, the inference is done by aggregating the ensembles, and uncertainty is obtained from the prediction variance (regression) or average entropy (classification). The second strategy is to construct different neural network architectures (number of layers, hidden neurons, type of activation functions.) [110]. This strategy can account for the uncertainty from model misspecification. Other strategies include different initialization of parameters along with a random shuffle of the datasets. This is better than the bootstrap strategy since more samples are utilized for each model. The third type is hyperensemble [177]. This approach constructs ensembles with different hyper-parameters, such as learning rate, optimization strategy, and training strategy.

Though the ensemble model is simple to the large dataset for modern neural networks, this method has several limitations: first, there is much *computational overhead*, since it requires training multiple independent networks and needs to keep all these networks in memory during inference. Second, *model diversity* is a necessary requirement for ensuring the diversity of the ensemble models to provide accurate uncertainty estimation. Otherwise, the ensemble model can collapse to the same local minima.

5.1.3 Sample distribution-related methods. In Section 3.1.1, we described model uncertainty related to sample distribution as a third category. It further includes two cases: (1) test samples and training samples follow different distributions (out of distribution); (2) a test sample is far away from other training samples (or is surrounded by sparse training samples) in the feature space. Here we only review methods in the case (2), i.e., sample density (distance)-aware neural networks. We do not specifically discuss out-of-distribution (OOD) methods as BNNs and ensemble methods can also be used for OOD-related uncertainty. We will review the methods for OOD problems in Section 6.

Because of the theoretical soundness of the BNN model and the simplicity of deep ensemble models, they are the popular methods for modern DNN uncertainty quantification. However, the *computational challenge* with BNN and ensemble models make it infeasible for real-world applications. In addition, the approaches can address the model uncertainty associated with the parameter, model architecture, and training process stochasticity, but cannot generalize to model uncertainty coming from *low sample density*, which means, the samples lie far away from the support of the training sets may show over-confident results. In this regard, many approaches have been motivated to develop sample density-aware neural networks to capture the model uncertainty due to low training sample density. Existing work can be summarized into two categories: Gaussian process hybrid neural network and distance-aware neural network. Each category will be discussed in the following.

Gaussian Process Hybrid Neural Network:

Summary on Gaussian process: Gaussian process (GP) is a variant of stochastic process, where any finite collection of random variables follow a multivariate Gaussian distribution [178]. Given a set of points $\{\boldsymbol{x}_i\}_{i=1}^n$, a GP defines a prior over functions $y_i = f(\boldsymbol{x}_i)$, and assumes the $p(y_1, ..., y_n)$ follow the Gaussian distribution $\mathcal{N}(\boldsymbol{\mu}(\boldsymbol{x}), \Sigma(\boldsymbol{x}))$, where$\boldsymbol{\mu}(\boldsymbol{x})$ is the mean function, and $\Sigma(\boldsymbol{x})$ is the covariance function, given with $\Sigma_{ij} = \kappa(\boldsymbol{x}_i, \boldsymbol{x}_j)$. κ is a positive definite kernel function (radial basis function), that measures the similarity between any pairs of input samples. The kernel function also plays a role in controlling the smoothness of the GPs. For GP inference, given the new sample $\boldsymbol{x}_*$, the joint distribution between the new sample prediction y_* and training samples target variable y has the form as Eq 9 shows. $\mathbf{K}_n$ is the covariance matrix between n training samples and $\mathbf{K}_{\boldsymbol{x}}$ is the covariance between the test sample and training samples. K_* is the prior variance of the test sample.

$$\begin{pmatrix} \mathrm{y} \\ y_* \end{pmatrix} = \mathcal{N}\left(\begin{pmatrix} \boldsymbol{\mu} \\ \mu_* \end{pmatrix}, \begin{pmatrix} \mathbf{K}_n & \mathbf{K}_{\boldsymbol{x}} \\ \mathbf{K}_{\boldsymbol{x}}^T & K_* \end{pmatrix} \right) \tag{9}$$

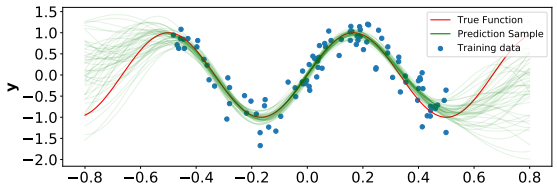

Fig. 7. Gaussian Process inference example: green lines are the prediction sample distribution

Then the prediction on new test input sample $\boldsymbol{x}_*$ is through computing the posterior distribution conditioned on the training data $\mathcal{D}_{\text{tr}}$, given by Eq. 10. GP inference gives lower uncertainty if the test samples are around the region where training samples are abundant (higher sample density as in the middle part of Fig. 7), otherwise resulting in higher uncertainty (boundary part of Fig. 7). Note that even Gaussian Process belongs to Bayesian methods, it considers the uncertainty source different from the BNN methods, For the Gaussian process method, it captures the uncertainty related to sample sparsity. Thus, we categorize GP as a different submodule to BNN methods.

$$p(y_*|x_*, \mathcal{D}_{\text{train}}, \boldsymbol{\theta}) = \mathcal{N}(y|\mathbf{K}_{\boldsymbol{x}}^T \mathbf{K}_n^{-1} \boldsymbol{y}, K_{x*} - \mathbf{K}_{\boldsymbol{x}}^T \mathbf{K}_n^{-1} \mathbf{K}_{\boldsymbol{x}}), \tag{10}$$

Sparse Gaussian process: Though possessing the intriguing property of inherent uncertainty estimation, GP is prohibitive for large datasets because the inversion of covariance matrix requires $O(n^3)$ complexity (n is the total number of training samples), which takes high computation and storage cost for training and inference on large datasets. In this regard, many methods [158, 166]attempt to make a sparse approximation to the full GP to bring down the computation to $O(m^2 n)$ (m is the number of inducing variables and $m \ll n$. The inducing variables can be anywhere in the input domain, not constrained to be a subset of the training data, which is denoted as input-output pairs $\{\hat{\boldsymbol{x}}_i, \hat{y}_i\}_{i=1}^m$. Then the inversion of the original covariance matrix $\mathbf{K}_n$ can be replaced with a low-rank approximation from the inducing variables, which only requires the inversion of $m \times m$ matrix $\mathbf{K}_m$. Then the question becomes how to select m best-inducing variables to be representative of the training dataset. Common approaches assume that the best representative inducing variables are those that maximize the likelihood (ML) of the training data [158]. Then the location of inducing variables and hyper-parameters of GP are optimized simultaneously through ML. The training data likelihood can be obtained by marginalizing the inducing variables on the joint distribution of training data and inducing variables. Another approach variation sparse GP formulates a variation lower bound of the exact likelihood by treating the locations of inducing

variables as variational parameters [166] for optimization. To further reduce the computation for more scalable inference on a large dataset, the paper [179] proposes a kernel interpolation method for scalable structured GP method by exploiting the structure of the covariance by imposing grid constraint on the inducing variables. In this way, the kernel matrix $\mathbf{K}_m$ admits the Kronecker structure and is much easier for computing the inversion.

Deep Gaussian process: Besides the computational challenge, another limitation of GP is the joint Gaussian distribution assumption on the target variables limits the model's capability in capturing diverse relationships among instances in large datasets. Additionally, GP relies heavily on the kernel function to compute the similarity between samples by transforming input features into the high-dimensional manifold. However, for high-dimension structured data, it is challenging to construct appropriate kernel functions to extract hierarchical features for computing similarity between samples. To address these limitations, two lines of research areas have been proposed: *deep kernel learning* and *Deep Gaussian process*.

Deep kernel learning [180] aims to combine the structured feature learning capability of DNN with the GP to learn more flexible representations. The motivation is that DNN can automatically discover meaningful representations from high-dimensional data, which could alleviate the fixed kernel limitations of GP and improve its expressiveness. Specifically, the deep kernel learning transforms the kernel $\mathbf{K}_{\boldsymbol{\theta}}(\boldsymbol{x}_i, \boldsymbol{x}_j)$ to $\mathbf{K}_{\boldsymbol{\theta}}(g(\boldsymbol{x}_i;\boldsymbol{w}), g(\boldsymbol{x}_j,\boldsymbol{w}))$, where $g(\cdot;\boldsymbol{w})$ is the neural network parameterized with $\boldsymbol{w}$ and $\mathbf{K}_{\boldsymbol{\theta}}$ is the base kernel function (e.g., radial basis function) of GP. The deep learning transformation can capture the non-linear and hierarchical structure in high-dimensional data. The GP with the base kernel is applied on the final layer of DNN and makes inference based on the learned latent features as Fig. 8 (a) shows. The idea has been successfully applied to spatio-temporal crop yield prediction where GP plays a role in accounting for the spatio-temporal auto-correlation between samples [187], which cannot be reflected from the DNN features.

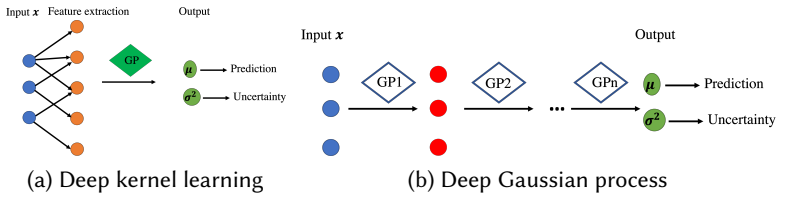

(a) Deep kernel learning (b) Deep Gaussian process

Fig. 8. Illustration of model uncertainty

The other category of deep GP is *compositional Gaussian process* [33] and focuses on function composition inspired by the architecture of deep neural networks. In this model, each layer is a GP model, whose inputs are governed by the output of another GP as Fig. 8 (b) shows. The recursive composition of GPs results in a more complex distribution over the target variables prediction. which overcomes the joint Gaussian distribution limitation of vanilla GP. The forward propagation and joint probability distribution can be written as:

$$\boldsymbol{y} = \boldsymbol{f}_L(\boldsymbol{f}_{L-1}(...\boldsymbol{f}_1(\boldsymbol{x}))) \text{ and } p(y, \boldsymbol{f}_L, ...\boldsymbol{f}_1|\boldsymbol{x}) \sim p(\boldsymbol{y}|\boldsymbol{f}_L)\prod_{i=2}^{L} p(\boldsymbol{f}_i|\boldsymbol{f}_{i-1})p(\boldsymbol{f}_1|\boldsymbol{x}) \tag{11}$$

where each function $\boldsymbol{f}_i(\cdot)$ is a Gaussian process model. The intermediate distribution follows the Gaussian distribution, but the final distribution will capture a more complex distribution over the target variable $\boldsymbol{y}$. The composition also allows the uncertainty to propagate from input through each intermediate layer. However, the challenge associated with the compositional Gaussian process

is: to maximize the data likelihood over $p(\boldsymbol{y}|\boldsymbol{x})$, the direct marginalization of hidden variables $\boldsymbol{f}_i$ are intractable. To overcome this challenge, variational inference by introducing inducing points on each hidden layer and optimizing over the variational distribution $q(\boldsymbol{f}_i)$. Then the marginal likelihood lower bound can be obtained by forwarding the variational propagation at each layer [168]. The framework also allows for incorporating partial or uncertainty observations into the model by placing a prior over the input variables $\boldsymbol{x}$ and propagating uncertainty layer by layer [34].

Table 2. Model uncertainty methods comparison

Model	Approach	Pros	Cons
BNN: **Pros**: Capture parameter uncertainty **Cons**: High computational costs	Variational inference [106, 139]	More flexible in the variational distribution format	Need approximation on the covariance format to trade off the computation.
	Laplace approximation [88, 146, 147]	Do not impact the neural network performance.	Need approximation in the covariance format and cannot capture the multi-modality posterior
	MCMC approximation [124, 151, 181]	Converge to exact posterior. No strict assumption on the distribution form.	Hard to converge
	MC dropout [50, 59]	Simple and compatible to modern neural network.	Lack rigorous theoretical analysis
Ensemble **Pros**: Capture model uncertainty from multiple perspectives. **Cons**: High computational and storage cost.	Network ensemble [110]	Capture uncertainty from the misspecification of model architecture.	Need to design various network architecture
	Bootstrap ensemble [90]	Capture uncertainty from low training dataset.	Use fewer datasets for training.
	Hyper-ensemble [177]	Capture uncertainty from training hyperparameters.	Hard to choose suitable hyperparameters for UQ.
Sample distribution **Pros**: Capture dataset shift uncertainty. **Cons**: Hard to ensure certain properties	Deep Gaussian process [33, 180, 187]	Leverage the capability of Gaussian process and DNN model.	The computation complexity for inference is high.
	Distance-aware DNN [101, 169, 170]	Ensure the hidden feature distance reflect sample distance in the feature space.	Hard to ensure the bi-Lipschit constraints.

Distance-aware neural network: Though modern neural networks have the capability of extracting representative features from large datasets, they are not aware of the extent of the distinction of new test samples to the training datasets. Thus, to characterize the uncertainty resulting from sample feature density, many approaches aim to take the distance awareness between samples into the design process of neural network motivated by Gaussian process [101]. Assume the input data manifold is equipped with a metric $||\cdot||_{\mathcal{X}}$, which can quantify the distance between samples in the feature space. The intuition of a distance-aware neural network is to leverage the feature extraction capability of DNN to learn a hidden representation $h(\boldsymbol{x})$ that reflects a meaningful distance in the data manifold $||\boldsymbol{x} - \boldsymbol{x}'||_{\mathcal{X}}$ as shown in Fig 9. However, one significant issue with the unconstrainted DNN model is the *feature collapse*, which means DNN feature extraction can map *in-distribution* data (training samples) and *out-of-distribution* data (lies further to the training data) to similar latent representations. Thus the Gaussian process based on the DNN extracted feature can be over-confident for those samples that lie further away from training samples.

To avoid the feature collapse problem, several constraints have been proposed on the models: sensitivity and smoothness [169, 170]. Sensitivity means a small change in the input should result in small changes in the feature representation, which can ensure distinct samples are mapped to

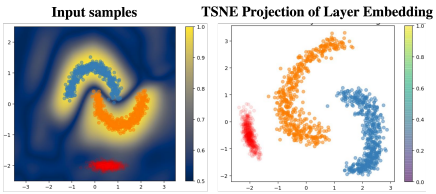

Fig. 9. Illustration on distance-aware neural network feature learning (adapted from [101])

different latent features. Smoothness means small changes in the input cannot lead to a dramatic transformation in the output. In general, these two constraints can be ensured by the *bi-Lipschitz* constraints [102], which means the relative changes in the hidden feature representation $h_{\boldsymbol{\theta}}(\boldsymbol{x})$ is bounded by the changes in input space as Eq. 12 shows.

$$L_1 * |\boldsymbol{x} - \boldsymbol{x}'|_{\mathcal{X}} < |h_{\boldsymbol{\theta}}(\boldsymbol{x}) - h_{\boldsymbol{\theta}}(\boldsymbol{x}')|_{\mathcal{H}} < L_2 * |\boldsymbol{x} - \boldsymbol{x}'|_{\mathcal{X}} \tag{12}$$

To enforce bi-Lipschitz constraints to DNN, two approaches have been proposed: spectral normalization and gradient penalty. Spectral normalization [101] claims that the bi-Lipschitz constants L can be ensured to be less than one by normalizing the weights matrix in each layer with the spectral norm. This method is fast and effective for practice implementation. The other approach is called gradient penalty [170], which introduces another loss penalty: the square gradient at each input sample $\nabla^2_{\boldsymbol{x}} h_{\boldsymbol{\theta}}(\boldsymbol{x})$. This will add a soft constraint to the neural networks to constrain the Lipschitz coefficients. Compared to spectral normalization, gradient penalty is a soft constraint and takes more computation to implement.

5.1.4 Summary on Model Uncertainty: We summarize and compare existing methods for quantifying uncertainty arising from model uncertainty. The advantages and disadvantages of each method are concluded in Table 2. BNN model can capture model uncertainty arising from parameter estimation but usually has high computational costs. The ensemble models can capture uncertainty from multiple perspectives, such as model architecture misspecification, low training dataset, and hyperparameters. The method also has a high computational cost. On the other hand, the sample distribution-based model can capture dataset shift uncertainty, but it's often hard to learn the distance-aware feature space and need to add constraints to the neural network model.

5.2 Data Uncertainty

In this section, we discuss the existing methodologies that quantify the data uncertainty for DNN models. Generally speaking, data uncertainty is represented by the distribution $p(y|\boldsymbol{x}, \boldsymbol{\theta})$, where $\boldsymbol{\theta}$ is the neural network parameters. To learn this distribution, we categorize the approach into deep discriminative models and deep generative models. Deep discriminative models are further divided into parametric and non-parametric models based on the distribution format. Deep generative models are divided into VAE-based and GAN-based models according to the generative frameworks.

5.2.1 Deep discriminative model . To quantify the data uncertainty, a discriminative model directly outputs a predictive distribution with a neural network. Specifically, the distribution can be represented by a parametric or non-parametric model. The parametric model assumes the output follows an explicit parameterized family of probability distributions whose parameters (e.g., mean and variance for Gaussian distribution) are predicted with the neural network while the non-parametric model does not have any assumption on the underlying distributions. We will discuss existing works for each category in detail.

Parametric model: The standard approach for quantifying data uncertainty is directly learning a parametric model for $p(y|\boldsymbol{x}, \boldsymbol{\theta})$. From a frequentist view, there exists a single set of optimum parameters $\boldsymbol{\theta}*$. For the classification problem, $p(y|\boldsymbol{x}, \boldsymbol{\theta})$ is a parameterized categorical distribution on the k class, and the distribution parameter $\boldsymbol{\pi} = (\pi_1, ..., \pi_K)$ are predicted from model output as Eq. 13 shows.

$$p(y|\boldsymbol{x}, \boldsymbol{\theta}) = \text{Categorical}(y; \boldsymbol{\pi}) \ , \ \boldsymbol{\pi} = f(\boldsymbol{x}; \boldsymbol{\theta}), \ \sum_{c=1}^{K} \pi_c = 1, \ \pi_c > 0 \tag{13}$$

In order to obtain the categorical distribution parameters, a straightforward method directly utilizes the softmax probability output as $\pi_i = \frac{\exp(h_i(x;\boldsymbol{\theta}))}{\sum_{c=1}^{k} \exp(h_c(x;\boldsymbol{\theta}))}$ as the predicted to indicate the uncertainty, but these methods tend to be over-confident because the softmax operation squeezes the prediction probability toward extreme values (zero or one) for the vast majority range of h_i [64]. Following work [59] calibrate the softmax uncertainty with *temperature scaling*, which simply add one more hyper-parameter T to the softmax calculation as $p = \frac{\exp(h_i(x)/T)}{\sum_{c=1}^{k} \exp(h_c(x)/T)}$ to overcome the overconfident outputs. This approach is straightforward to implement, but is still faced with the potential to be over-confident due to the lack of any constraints, and require calibration on the parameter.

For regression problems, data uncertainty is assumed to come from the inherent noise (or measurement error, human labeling error) in the training data. In general, the training data is modeled as independent additive Gaussian noise with sample-dependent variance $\sigma(\boldsymbol{x})$, which indicates the target variable $y_i = f_{\boldsymbol{\theta}}(\boldsymbol{x}_i) + \epsilon(\boldsymbol{x}_i)$. $\epsilon(\boldsymbol{x}_i)$ is the independent heterogeneous Gaussian noise, which represents the uncertainty for each sample. In this way, the output will be a parameterized continuous Gaussian distribution, as Eq. 14 and Fig. 10 (a) show. Both the mean and variance are predicted from the neural network [82]. The mean represents the prediction of the model and the variance represents the uncertainty of the sample prediction. To optimize the neural network parameters $\boldsymbol{\theta}$, maximize likelihood is performed on the mean and variance jointly as Eq. 14 shows. This is also known as heteroscedastic regression, which assumes the observational noise level varies with different samples. This is suitable for the case where some samples have higher noise (uncertainty), while others have lower. Besides Gaussian distribution, the neural network can be parameterized with many other kinds of distributions, such as mixture Gaussian distribution [58], which is implemented with mixture density network (MDN) [14], assuming multiple modes for the prediction. MDN has the advantage that can account for the uncertainty from multiple prediction modes but consumes more computation. It's important to choose a suitable parameterized distribution, which depends on the nature of the problem.

$$p(y|\boldsymbol{x}, \boldsymbol{\theta}) = \mathcal{N}(f_{\boldsymbol{\theta}}(\boldsymbol{x}), \sigma_{\boldsymbol{\theta}}(\boldsymbol{x})) \ \text{ and } \ \mathcal{L}_{\text{NN}}(\boldsymbol{\theta}) = \frac{1}{n} \sum_{i=1}^{n} \frac{1}{2\sigma_{\boldsymbol{\theta}}^2(\boldsymbol{x}_i)} ||y_i - f_{\boldsymbol{\theta}}(\boldsymbol{x}_i)||^2 + \frac{1}{2} \log \sigma_{\boldsymbol{\theta}}^2(\boldsymbol{x}_i) \tag{14}$$

The advantage of prediction distribution is that it is simple to add the approach to existing neural network architecture and requires little modification to the training and inference process. However, the explicit parameterization form requires choosing the appropriate distribution to accurately capture the underlying uncertainty, which can be hard if no prior information is available.

Non-parametric model: Another widely popular approach to indicate the data uncertainty is through *prediction interval* (PI) [136, 182]. For regression problems, the prediction intervals output a lower and upper bound $[y_l, y_u]$, with which we expect the ground truth y falls into the interval with a prescribed confidence level, $1 - \alpha$, meaning that $p(y \in [y_l, y_u]) > 1 - \alpha$ as shown in Fig. 10 (b). This approach does not require explicit distribution over the prediction variable and is more flexible. Traditional prediction intervals are constructed in two steps, First step is to learn the point estimation of the target variable, which is obtained through the minimization of the error-based

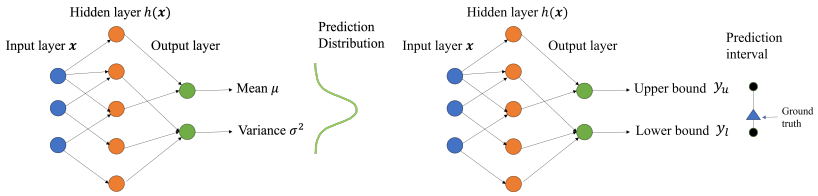

(a) Prediction distribution example (b) Prediction interval example

Fig. 10. Neural network architecture for parametric and non-parametric model

loss function (i.e., mean square loss), and then estimate the prediction variance around the local optimum prediction. The strategy is trying to minimize the prediction error, but not optimize the prediction interval quality. One recent paper explicitly constructs a lower and upper bound estimation (LUBE) to improve the PI characteristics, i.e., the width and coverage probability. The basic intuition is that the PI should cover the ground truth with a certain pre-defined probability (confidence level), but should be as narrow as possible. The approach improves the quality of the constructed PI, but the new cost function is non-differentiable and requires Simulated Annealing (SA) sampling to obtain the optimal NN parameters.

To overcome the non-differentiable limitation of LUBE, another approach proposes a coverage width-based loss function [136] with a similar goal as LUBE, shown in the Eq.15. The *mean prediction interval width* (MPIW) is equal to $|y_u - y_l|$, and *prediction interval coverage width* (PICP) indicates the average probability that the PI covers the ground truth. The total loss encourages the PI to be narrow while having a higher coverage probability than the prescribed confidence level α.

$$\text{Loss} = \text{MPIW} + \lambda * \max(0, (1-\alpha) - \text{PICP})^2 \tag{15}$$

Recent approaches put forward the method of prediction interval learning as an empirical constrained optimization problem. There are two different views of this optimization problem: primal and dual perspectives. The primal perspective views the optimization objective as minimizing the PI intervals under the constraints that the PI attains a coverage probability larger than the confidence level [25], which is expressed as follows:

$$\min_{L,U \in \mathcal{H}, L<U} \mathbb{E}_{\boldsymbol{x} \sim \pi(\boldsymbol{x})}(U(\boldsymbol{x}) - L(\boldsymbol{x}))\ s.t.\ p_\pi(y \in [L(\boldsymbol{x}), U(\boldsymbol{x})]) > 1-\alpha \tag{16}$$

where $\mathbb{E}_{\boldsymbol{x} \sim \pi(\boldsymbol{x})}$ denotes the expectation with respect to the marginal distribution of input samples $\boldsymbol{x}$, and p_π denote the probability of input and output pair distribution. To enforce the optimality and feasibility of the optimization problem, the tradeoff is developed through the studying of two characteristics of this approach: Lipschitz continuous model class [172] and Vapnik–Chervonenkis (VC)-subgraph class [25]. On the other hand, the dual perspective constructs the learning objective as maximizing the PI coverage probability under the fixed global budget constraints (average PI width) in a batch setting [149].

$$\min_{f \in \mathcal{F}} \mathbb{E}_{(\boldsymbol{x},y) \sim \pi(\boldsymbol{x},y)} L(y, U(\boldsymbol{x}), L(\boldsymbol{x}))\ s.t.\ \sum_i (U(\boldsymbol{x}_i) - L(\boldsymbol{x})_i) < B \tag{17}$$

They presented a discriminative learning framework that optimizes the expected error rate under a budget constraint on the interval sizes. In this way, the approach avoids single-point loss and can provide a statistical guarantee of the generalization capability of the whole population. Compared with the primal setup, the dual perspective in batch learning can construct the prediction interval of a group of test points at the same time and avoid the computational overhead.

5.2.2 Deep Generative Model. The deep generative model (DGM) is a family of probabilistic models that aim to learn the complicated, high-dimensional data distribution $p_{\text{data}}(\boldsymbol{x})$ with DNN. DGMs are capable of learning the intractable data distribution in the high-dimensional feature space $\mathcal{X} \in \mathbb{R}^n$ from a large number of independent and identical observed samples $\{\boldsymbol{x}_i\}_{i=1}^m$. Specifically, they learn a probabilistic mapping from some latent variables $\boldsymbol{z} \in \mathbb{R}^d$ which following tractable distribution to the data distribution, e.g., $\mathcal{N}(\mathbf{0}, \mathbf{I})$ to the data distribution $p_{\text{data}}(\boldsymbol{x})$. Mathematically, the generative model can be defined as a mapping function $g_{\boldsymbol{\theta}}(\cdot) : \mathbb{R}^d \rightarrow \mathbb{R}^n$, where d and n are the dimensions of latent variable and original data, respectively. The ability of the deep generative model to learn an intractable distribution makes it useful for uncertainty quantification.

The basic idea is to employ DGM to learn the *predictive distribution* $p(y|\boldsymbol{x})$ given the supervised training data pairs $\{(\boldsymbol{x}_i, y_i)\}_{i=1}^m$. It should be noted that if we aim to learn the *predictive distribution* instead of the data distribution in feature space, the *conditional deep generative model* (cDGM) [159] should be employed. Generally speaking, cDGM-based uncertainty quantification models learn a conditional density over the prediction y, given the input feature $\boldsymbol{x}$. This amounts to learn a model $g_{\boldsymbol{\theta}}(\boldsymbol{z}, \cdot) : \mathbb{X} \rightarrow \mathbb{Y}$ such that the generative model $g(\boldsymbol{z}, \boldsymbol{x})$ with $\boldsymbol{z} \sim p(\boldsymbol{z})$ is approximately distributed as the true unknown distribution $p_{\text{true}}(y|\boldsymbol{x})$. The variability of the prediction distribution $p(y|\boldsymbol{x})$ is encoded into the latent variable $\boldsymbol{z}$ and the generative model. During inference, for any $\boldsymbol{x} \in \mathbb{X}$, we can generate m samples with $y_i = g_{\boldsymbol{\theta}}(\boldsymbol{z}_i, \boldsymbol{x})$ and $\boldsymbol{z}_i \sim p(\boldsymbol{z})$ and from the samples $\{y_i\}_{i=1}^m$ the variability we can quantify the prediction uncertainty.

In the following subsection, we consider two types of deep generative models: variational auto-encoder (VAE) [84] and generative adversarial network (GAN) [56]. VAE belongs to the likelihood-based generative model and is trained via maximizing evidence lower bound (ELBO) of the likelihood function. The GAN model is an implicit generative model trained with a two-player zero-game approach. We will consider how the two frameworks could be utilized for prediction uncertainty estimation.

VAE-based model: VAE model consists of two modules: an *encoder* and a decoder. The encoder network $q_{\boldsymbol{\phi}}(\boldsymbol{z}|\boldsymbol{x})$ aims to embed the high dimensional structural output $\boldsymbol{x}$ into a low-dimensional code $\boldsymbol{z}$, that capture the inherent ambiguity or noise of the input data. The decoder $p_{\boldsymbol{\theta}}(\boldsymbol{x}|\boldsymbol{z})$ aim to reconstruct the input feature. VAE model has been popular for structured output uncertainty, especially for the tasks on image data, because of their capability to model the global and local structure dependency in regular grid images. Specifically, two kinds of frameworks based on the VAE model have been proposed to account for the data uncertainty coming from *input noise* and *target output noise*: The first category aims to capture the noise that lies in the input samples. The basic idea is to embed each sample as a Gaussian distribution instead of a deterministic embedding in the low dimensional latent space, where the mean represents the feature embedding and variance represents the uncertainty of the embedding [23]. The method takes into the different noise levels inherent in the dataset, which is ubiquitous in many kinds of real-world datasets, i.e., face image recognition [23], medical image reconstruction [45]. The probabilistic embedding framework takes advantage of the VAE model architecture to estimate the embedding and uncertainty simultaneously. The second category aims to capture the noise that lies in the target outputs, which also means the ground truth is imperfect, ambiguous, or corrupted. This scenario is common in the medical domain [92], where the objects in the image are ambiguous and the experts may not reach a consensus on the class of the objects (large uncertainty). Thus for segmentation or classification tasks, the model should be aware of the prediction uncertainty. To capture the prediction uncertainty in the target outputs, the conditional VAE (cVAE) [159]framework is adopted. Specifically, cVAE formulates the

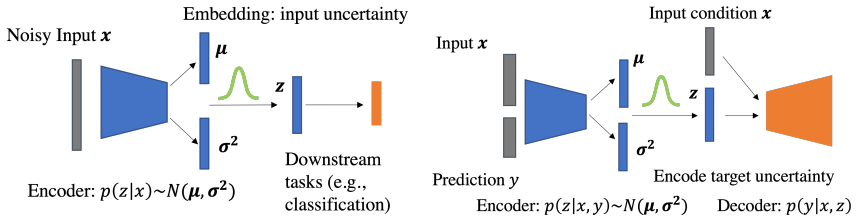

(a) Input uncertainty (b) Target prediction uncertainty

Fig. 11. VAE framework for uncertainty quantification

prediction distribution as an integration over the latent embedding z,

$$p(y|\boldsymbol{x}) = \int p(y|\boldsymbol{x}, z)p(z|\boldsymbol{x})dz \approx \sum_{j=1}^{n} p(y|\boldsymbol{x}, z_j), \text{ where } z_j \sim p(z) \tag{18}$$

The cVAE model is trained by maximizing the evidence lower bound of the likelihood. Then during inference, multiple latent feature z_j can be drawn from the prior distribution, and the integration over latent z can be approximated with the sampling distribution [140]. Probabilistic U-Net model [85] combines the architecture of cVAE and U-Net model by treating the U-Net model as the encoder to produce a probabilistic segmentation map. The U-Net model can capture multi-scale feature representations in the low-dimensional latent space to encode the potential variability in the segmentation map. These types of models are illustrated in Fig. 11 (a) and (b).

In summary, the VAE-based framework can take into consideration the data uncertainty coming from the input noise or the target output noise and can adapt the current state-of-the-art neural network architecture into its framework, making it more flexible for many kinds of applications. The key success lies in modeling the joint probability of all samples (pixels) in the image. The approach is suitable for structured uncertainty quantification (e.g., image grid structure, graph structure, et al.) through learning the implicit joint distribution of the structure.

GAN-based generative model: GAN is a type of generative model trained with a two-player zero-game. It consists of a *generator* and a *discriminator*. In conditional GAN (cGAN), the generator takes the input x and random noise z as input and generates the target variables y: $\mathcal{G} : (\boldsymbol{x}, z) \rightarrow y$. The discriminator is trained to distinguish the generated samples and ground-truth samples. The idea has been adopted in many domains. For example, in the transportation domain, they adpot a GAN-based approach for the prediction of traffic vollume [118]. the flow model is integrated into GAN to enable likelihood estimation and better uncertainty quantification. Another approach [51, 128] further extends the method by utilizing the Wasserstein GAN [7] based on gradient penalty to improve model convergence. The key advantage of deep generative modeling for uncertainty quantification is that they directly parameterize a deep neural network to represent the prediction distribution, without the need to have an explicit distribution format. Moreover, it can integrate a physics-informed neural network for better uncertainty estimation of physical science [35]. However, the disadvantage is that deep generative models are much harder to train, especially for GAN-based models. The convergence of the model learning is not guaranteed.

Table 3. Data uncertainty methods comparison

Model	Approach	Pros	Cons
Deep Discriminative model **Pros**: compatible to existing network architecture. **Cons**: Hard for structured uncertainty	Parametric: predictive distribution [58, 82]	Can leverage existing DNN training framework.	Need to choose appropriate parametric distribution.
	Non-parametric: predictive interval [25, 136, 149, 182]	No need to choose specific distribution format.	Need to design new loss/training strategy.
Deep Generative model **Pros**: Capture structured uncertainty. **Cons**: Require modification to existing architecture and hard to train	VAE-based model [23, 45, 85, 140]	Capture the structured data uncertainty from the input noise and ambiguous label.	Need to modify neural network architecture
	GAN-based model [51, 118, 128]	Capture the structure data uncertainty.	GAN model is hard to train.

5.3 Model and data uncertainty

Besides considering the data and model uncertainty separately, many frameworks attempt to jointly consider the two kinds of uncertainty for more accurate quantification. In this part, we will review existing that aims to quantify two types of uncertainty simultaneously.

5.3.1 Approaches combining data and model uncertainty. A straightforward way to consider both data and model uncertainty is to select one of the approaches in each category and combine them in a single framework. Below we will introduce some major ways to combine the approach of data and model uncertainty and their potential drawbacks.

Combine BNN model with prediction distribution: The method aims to capture both data and model uncertainty in a single framework [82] by combining the BNN and prediction distribution. The model uncertainty is captured with the BNN approximation approach. Specifically, MC dropout is adopted due to its simplicity for implementation. For each dropout forward pass, one sample of the weight is drawn from the weight distribution approximation $\mathbf{W}_t \sim \text{Bernoulli}(p)$, where p is the dropout rate, then one forward prediction can be made with the weight by $y_t = p(y|\boldsymbol{x}, \mathbf{W}_t)$. To obtain the data uncertainty, the output is formulated as a parameterized Gaussian distribution instead of point estimation $[y_t, \sigma_t^2] = p(y|\boldsymbol{x}; \mathbf{W}_t)$, where y_t is the target variable mean prediction and σ_t^2 is the prediction variance for a single forward prediction. With multiple dropout forward passes, we have a set of T prediction samples $\{y_t, \sigma_t^2\}_{t=1}^T$. The predictive uncertainty in the combined model can be approximated with the law of total variance expressed as $\text{Var}(y)$ in Eq. 19. The intuition of this equation is that the total uncertainty comes from two parts, the last $\frac{1}{T}\sum_{t=1}^T \sigma_t^2$ represents the average data uncertainty, and the first part $\frac{1}{T}\sum_{t=1}^T y_t^2 - (\frac{1}{T}\sum_{t=1}^T y_t)^2$ represent the disagreement of T MC-dropout models, which capture the model uncertainty.

$$\text{Var}(y) \approx \frac{1}{T}\sum_{t=1}^{T} y_t^2 - (\frac{1}{T}\sum_{t=1}^{T} y_t)^2 + \frac{1}{T}\sum_{t=1}^{T} \sigma_t^2 \tag{19}$$

Combine ensemble model with prediction distribution: This approach [90] combines the ensemble method with prediction distribution. The deep ensemble method constructs an ensemble of DNN models $\mathcal{M} = \{\mathcal{M}_i\}_{i=1}^K$, where each model $\mathcal{M}_i$ can be set with different parameters, or architectures choices, et, al. The model uncertainty is expressed as the variance or "disagreement" of the ensemble. In this way, the output of each model is modified as a parameterized distribution to capture the data uncertainty. Similar to MC-dropout, we have an ensemble of prediction distribution $\{p(y|\boldsymbol{x}, \mathcal{M}_i)\}_{i=1}^K$. In this part, we take the classification problem as an example, where the prediction distribution is a parameterized categorical distribution. The total uncertainty is captured with the

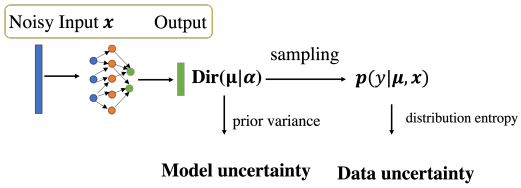

Fig. 12. Evidential deep learning architecture

entropy of average prediction distribution $\mathcal{H}(\mathbb{E}_{p(\mathcal{M}_i)}p(y|\boldsymbol{x}, \mathcal{M}_i))$, and the data uncertainty is the average entropy of each model, expressed as $\mathbb{E}_{p(\mathcal{M}_i)}\mathcal{H}(p(y|\boldsymbol{x}, \mathcal{M}_i))$. The model uncertainty can be expressed with the mutual information between the prediction and the ensemble model $y, \mathcal{M}$ as expressed in Eq. 20.

$$\text{MI}(y, \mathcal{M}) = \mathcal{H}(\mathbb{E}_{p(\mathcal{M}_i)}p(y|\boldsymbol{x}, \mathcal{M}_i)) - \mathbb{E}_{p(\mathcal{M}_i)}\mathcal{H}(p(y|\boldsymbol{x}, \mathcal{M}_i)) \tag{20}$$

Combine ensemble model with prediction interval: Since the prediction interval constructed in some approaches accounts only for the data noise variance, not the model uncertainty. To improve the total uncertainty estimation, ensemble methods are adopted to combine with prediction interval to account for the model uncertainty that comes from model architectures misspecification, parameter initialization, et.al. [136]. Specifically, Given an ensemble of models trained with different model specifications or sub-sampling of training datasets, where the model prediction intervals are denoted as $[y_l^{ij}, y_u^{ij}]$ for sample $i = \{1, ..., n\}$ and model $j = \{1, ..., m\}$, the model uncertainty can be captured by the variance of the lower bound $\sigma_l^{(i)^2}$ and upper bound variance $\sigma_u^{(i)^2}$. For example, the lower bound uncertainty is:

$$\begin{aligned}
\sigma_l^{(i)^2} &= \frac{1}{m-1}\sum_{j=1}^{m}(y_l^{(ij)} - \hat{y}_l^{(i)})^2, \text{ where } \hat{y}_l^{(i)} = \frac{1}{m}\sum_{j=1}^{m} y_l^{(ij)} \\
\sigma_u^{(i)^2} &= \frac{1}{m-1}\sum_{j=1}^{m}(y_u^{(ij)} - \hat{y}_u^{(i)})^2, \text{ where } \hat{y}_u^{(i)} = \frac{1}{m}\sum_{j=1}^{m} y_u^{(ij)}
\end{aligned} \tag{21}$$

Then the new prediction interval $[\tilde{y}_l, \tilde{y}_u]$ with 95% confidence level can be constructed as:

$$\tilde{y}_l = y_l - 1.96\sigma_l^{(i)^2}, \text{ and } \tilde{y}_u = y_u + 1.96\sigma_u^{(i)^2} \tag{22}$$

The constructed interval can reflect both the data uncertainty and model uncertainty, but the limitation is that the model uncertainty is simply constructed from the variance of the lower and upper bound of the ensemble, which lacks theoretical justification because of the independent consideration of two boundaries. To overcome this limitation, one recent approach proposes a split normal aggregation method to aggregate the prediction interval ensembles into final intervals [150]. Specifically, the method fits a split normal distribution (two pieces of normal distribution) over each prediction interval, and then the final prediction will become a mixture of split normal distribution. The PI can be derived from the $1 - \alpha$ quantile of the cumulative distribution.

In conclusion, to capture both the data and model uncertainty, existing literature can combine the methodologies in the two categories. There are several limitations to the combination approaches: first, the BNN or ensemble models require multiple forward passes for the prediction, which introduces computation overhead and extra storage. Efficiency is a concern. Second, the simple combination of data and model uncertainty lacks a theoretical guarantee, which requires post hoc calibration on the model.

5.3.2 Evidential deep learning. To overcome the computational challenge for the combination approaches, evidential deep learning was proposed to use one single deterministic model to capture both the data and model uncertainty without multiple forward passes of the neural network [9, 24, 109, 152]. The intuition of evidential deep learning is to predict class-wise evidence instead of directly predicting class probabilities. In the following section, we review the methodologies and their advantages and disadvantages.

As discussed in the aforementioned sections, for classification problems, existing Deep learning-based models explicitly or implicitly predict class probabilities (categorical distribution parameters) with softmax-layer parameterized by DNNs to quantify prediction uncertainty. However, the softmax prediction uncertainty tends to be over-confident [64]. Evidential deep learning is developed to overcome the limitation by introducing the evidence theory [78] to neural network frameworks. The motivation of evidential deep learning is to construct predictions based on evidence and predict the parameters of Dirichlet density. For example, considering the 3-class classification problem, a vanilla neural network directly predicts the categorical distribution on the class $\pi = \pi_1, \pi_2, \pi_3$ with $\sum_i \pi_i = 1$. However, this approach can only represent a point estimation of prediction distribution. On the other hand, evidential deep learning aims to predict the *evidence* for each class $\boldsymbol{\alpha} = \{\alpha_1, \alpha_2, \alpha_3\}$ with the constraints $\boldsymbol{\alpha} > 0$, which can be considered as the parameters of Dirichlet distribution [152]. The framework is shown in Fig 12, where the output is the *evidence* $\boldsymbol{\alpha}$ for each class, and the prediction distribution is sampled from the Dirichlet distribution. The expected prediction distribution for each class is $p_i = \frac{\alpha_i}{\sum_{c=1}^{3} \alpha_c}$, whose entropy reflects the data uncertainty. On the other hand, the model uncertainty is reflected with the total evidence $\sum_i \alpha_i$, which means the more evidence we collect, the more confident the model is.

Mathematically, evidential deep learning aims to learn the prior distribution of categorical distribution parameters, which is represented by the Dirichlet distribution. The Dirichlet distribution is parameterized by its concentration parameters $\boldsymbol{\alpha}$ (evidence) where α_0 is the sum of all α_i and is referred to as the precision of Dirichlet distribution. A higher value of α_0 will lead to sharper distribution and lower model uncertainty. As shown in Eq.23, the $\mathrm{Dir}(\boldsymbol{\mu}|\boldsymbol{\alpha})$ defines a probability density function over the k-dimensional random variable $\boldsymbol{\mu} = [\mu_1, ..., \mu_k]$, where k is the number of classes, $\boldsymbol{\mu}$ belongs to the standard $k-1$ simplex ($\mu_1 + ... + \mu_k = 1$ and $\mu_i \in [0, 1]$ for all $i \in 1, ..., k$), and can be regarded as the categorical distribution parameters. The relationship between Dirichlet distribution and uncertainty quantification can be illustrated using a 2-simplex. The random variable $\boldsymbol{\mu} = [\mu_1, \mu_2, \mu_3]$ is represented by its Barycentric coordinates in Fig 13 on the 2-simplex. The Barycentric coordinate is a coordinate system where points are located inside a simplex, and the value in each coordinate can be interpreted as the fraction of masses placed at the corresponding vertices of the simplex. Fig 13 (a) shows a scenario where the evidence parameters are equal, resulting in three classes being indistinguishable and implying high data uncertainty (high entropy for the sampled $\boldsymbol{\mu}$). As the total evidence $\sum_i \alpha_i$ increases, the density becomes more concentrated, which means the model uncertainty decreases, while the data uncertainty remains fixed. Fig 13 (b) shows a scenario with fixed model uncertainty, as the sum of evidence parameters remains constant. When the evidence becomes imbalanced, the density becomes more concentrated toward one class, thus decreasing the data uncertainty.

$$\mathrm{Dir}(\boldsymbol{\mu}|\boldsymbol{\alpha}) = \frac{\mathrm{T}(\alpha_0)}{\prod_{c=1}^{K} \mathrm{T}(\alpha_c)} \prod_{c=1}^{K} \mu_c^{\alpha_c - 1}, \alpha_c > 0, \ \alpha_0 = \sum_{c=1}^{K} \alpha_c \tag{23}$$

Due to the intriguing property of Dirichlet distribution, evidential deep learning directly predicts the parameters of Dirichlet density. For example, the Dirichlet prior network (DPN) [109] learn the concentration parameter $\boldsymbol{\alpha}$ for the Dirichlet distribution $\boldsymbol{\alpha} = \boldsymbol{f}(\boldsymbol{x}, \boldsymbol{\theta})$. Then the categorical

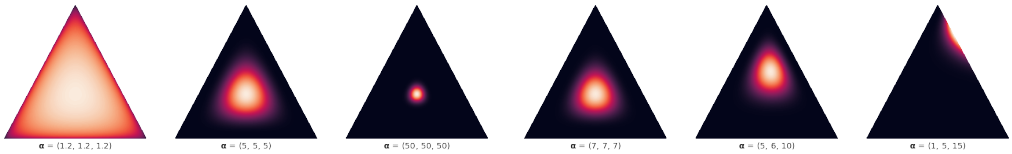

(a) Keep data uncertainty fixed , and model uncertainty decrease from left to right.

(b) Keep the model uncertainty fixed, and the data uncertainty decreases from left to right (the entropy of the categoric distribution decreases).

Fig. 13. Dirichlet distribution density visualization

distribution parameters can be drawn from the Dirichlet distribution as $p(\boldsymbol{\mu}|\boldsymbol{x}, \boldsymbol{\theta}) = \text{Dir}(\boldsymbol{\mu}|\boldsymbol{\alpha})$. The prediction of class probability is the average over possible $\boldsymbol{\mu}$.

$$p(w_c|\boldsymbol{x}, \boldsymbol{\theta}) = \int p(w_c|\boldsymbol{\mu}) p(\boldsymbol{\mu}|\boldsymbol{x}, \boldsymbol{\theta}) = \frac{\alpha_c}{\alpha_0} \tag{24}$$

To measure the uncertainty from the Dirichlet distribution, the total uncertainty is the entropy of the average prediction distribution, and data uncertainty is the average of the entropy in each realization of $\boldsymbol{\mu}$. Several approaches have extended the Prior network to a regression model and a posterior network has also been proposed for more reliable uncertainty estimation.

The advantage of evidential deep learning is the approach only requires a single forward pass during inference and is much more computationally efficient. The approach also explicitly distinguishes data and model uncertainty in a principled way. The disadvantage is that the training stage is more complicated and is not guaranteed to obtain the same or similar prediction accuracy with vanilla network and cannot leverage existing progress in DNN. Furthermore, the training stage requires OOD samples to learn well representations and increase the amount of dataset.

Table 4. Simultaneous Model and Data Uncertainty Methods Comparison

Model	Approach	Pros	Cons
Combination of existing approaches **Pros**: Easy to implement. **Cons**: High computation and storage cost.	Combine BNN with prediction distribution [82]	Capture uncertainty from both data noise and model parameters.	Require multiple forward pass during inference.
	Combine ensemble with prediction distribution [90]	Capture uncertainty from both data noise and mode architectures.	Require more computation and storage requirement.
	Combine ensemble with prediction interval [136, 150]	Capture both data and model uncertainty and do not need explicit parametric distribution form.	Require modification on existing DNN training process.
Evidential deep learning	Evidential deep learning [9, 24, 109, 152]	Capture both data and model uncertainty and Computationally efficient compared with BNN and ensemble methods	Strong assumption on prior distribution. Difficult to train compared with BNN or ensemble.
Conformal Prediction	Prediction set or interval [22, 62, 79, 107]	Capture both data and model uncertainty and Distribution free	Strong assumption on sample distribution.

5.3.3 Conformal Prediction. Though existing UQ approaches can quantify total uncertainty from different sources, the lack of formal guarantees is a major limitation in their methods. To address this issue, conformal prediction (CP) is a post-process approach by constructing a finite prediction set with the statistical guarantee to cover the true label [6].

Conformal prediction is a method of distribution-free uncertainty quantification, which is model-agnostic and provides formal results for marginal coverage, defined as the the average probability that the true class will be contained in the prediction set [5]. Formally, this coverage guarantee states:

$$\mathbb{P}(y \in C(x)) >= 1 - \alpha \tag{25}$$

where $\boldsymbol{x}$ is a sample instance, and y is the ground truth. Unlike traditional confidence intervals which typically assume a specific distribution of data or residuals, conformal prediction offers a non-parametric and distribution-free approach [79]. This is advantageous in deep learning, where the assumptions required by traditional methods are often violated due to the complexity and non-linearity of the models.

There are several approaches to developing conformal predictions for deep learning models. The first kind of approach is to apply the conformal method to pre-trained deep learning models directly [107]. Second, credal Bayesian deep learning trains an (uncountable) infinite ensemble of BNNs using only finitely many elements, and outputs a prediction set for total uncertainty estimation [22]. Third, density-based deep conform prediction considers the distance among samples to model the uncertainty coming from out-of-distribution aspects explicitly [62]. However, the limitation of conformal prediction in deep learning is that it depends on the assumption that the data instances are independently and identically distributed (i.i.d.) and exchangeable. This assumption is violated in many structured data, including spatiotemporal data, and graph data, where there exists structural dependency among samples.

5.3.4 Evaluation Metrics. The previous subsections discuss various approaches for model and data uncertainty quantification. In this part, we discuss how to evaluate the performance of an uncertainty quantification model. There are several metrics to evaluate the performance of uncertainty quantification from different perspectives. First, one method is to evaluate the calibration between the uncertainty measure and the fraction of correct prediction, called expected calibration error (ECE [121]). It first discretizes the uncertainty value into a fixed number of bins and assigns each predicted probability to the bin that encompasses it. The calibration error is the difference between the fraction of predictions in the bin that are correct (accuracy) and the mean of the probabilities in the bin (confidence). Given the groundtruth $\hat{y}$, the prediction from a model Y, and prediction uncertainty $\hat{p}$, the model is calibrated when the probability of being correct $\mathbb{P}(Y = \hat{y})$ is equal to the uncertainty measure $\hat{p}$:

$$\mathbb{P}(Y = \hat{y}|\hat{p}) = \hat{p} \text{ for any } \hat{p} \tag{26}$$

Second, to address any distortion of results introduced by the binning procedure, the smooth ECE (smECE [15]), which avoids the binning altogether by smoothing observations using an RBF kernel. Third, the area under the ROC (AUROC) [133] treats the problem as a binary misclassification by using uncertainty to predict the correctness of the prediction and aggregating the results over all possible decision thresholds. The intuition of this measure is that more uncertainty should indicate a lower probability of the correctness of the answers. Thus, AUROC measures the rank of the uncertainty score. Fourth, the Brier score is a strictly proper score function [19]. It measures the mean squared difference between the predicted probability and the actual outcome. Last, Adaptive

Calibration Error (ACE [127]) computes the calibration across all predictions for multi-classes to overcome the limitation of ECE.

6 UNCERTAINTY ESTIMATION IN VARIOUS MACHINE LEARNING PROBLEMS

In this section, we discuss several major ML problems where UQ can play a critical role. For each problem, we discuss the following four perspectives, including *the nature of the data* on the application, *the source of uncertainty*, *the challenges* associated with uncertainty quantification, and *the existing literature* for the specific problems.

6.1 Out-of-distribution detection

It is a fundamental assumption for a deep neural network that the test data distribution is similar to the training data distribution $p_{\text{train}}(x) \approx p_{\text{test}}(x)$. However, in real-world tasks, DNN can encounter many out-of-distribution (OOD) data, which come from some different distributions compared with the training data. DNN performance may drop significantly and give unreliable predictions in such situations. The model should be aware of such situations to avoid over-confident predictions.

Given a training data distribution $p(x)$, the OOD data are those samples that are either unlikely under the training data distribution or outside the support of $p(x)$. Accurate detection of OOD samples is of paramount importance for safety-critical applications, e.g., autonomous driving [153], medical image analysis [54] Since OOD samples lie further away from the training samples, the trained model may not generalize well and produces diverse and unstable predictions for those samples. The model parameters or architecture are not suitable for OOD samples. Thus OOD samples are expected to have higher model uncertainty. The primary uncertainty for OOD data is concerned with model uncertainty, because the model trained with in-distribution may not generalize well to other domains. It is important to make the model aware of the sample density when quantifying the uncertainty.

Existing approaches: From the above analysis we are clear that model uncertainty is more important for OOD detection. Thus existing approaches leveraging the model uncertainty framework are much more popular. For example, drop-out-based BNN approaches have been applied to OOD detection and improved the performance through the use of the randomized embeddings induced by the intermediate layers of a dropout BNN [125] and node-based BNN [167]; Deep ensembles are simple but perform well on OOD detection [90, 133, 188]. Recent advances attempt to develop distance-aware DNN for more accurate OOD detection by imposing constraints on the feature extracting process [101, 169]. Recent developments in evidential deep learning framework have also demonstrated its capability on OOD detection in many benchmark datasets because of the explicit distinction between two types of uncertainty in the framework [9, 24, 109, 152].

6.2 Active Learning

For the deep learning model, obtaining labeled data can be laborious, and time-consuming. Active learning [145] aims to solve the data labeling issue by learning from a small amount of data and choosing by the model what data it requires the user to label and retrain the model iteratively. The goal is to reduce the number of labeled examples needed for learning as much as possible, which means requiring a strategy to choose which sample is more worth labeling for the model. Utilizing predictive uncertainty has been a popular strategy and those instances whose prediction is maximally uncertain are most useful.

The key goal in active learning is to choose observations $\boldsymbol{x}$ for which obtaining labels y would improve the performance of the learning. As discussed in the background, adding samples with large data uncertainty cannot improve the trained model because its inherent randomness is irreducible while more samples with model uncertainty can improve the model performance. In this regard,

model uncertainty is more important for active learning [126]. The critical challenge for active learning is to distinguish between the data and model uncertainty and utilize model uncertainty for selecting new samples.

Existing approaches: Similar to OOD detection, the approaches for model uncertainty detection can be adapted to an active learning framework by considering uncertainty coming from the parameter, model architecture, and sample density sparsity. For example, the BNN framework considers the samples that decrease the entropy of $p(\boldsymbol{\theta}|\mathcal{D}_{\text{tr}}, \{\boldsymbol{x}, y\})$ most will be most useful [41]. The deep ensemble and MC-dropout approach can also be a straightforward way for quantifying the model uncertainty in active learning [63]. Recent approaches propose margin-based uncertainty sampling scheme and provide convergence analysis [142]

6.3 Deep Reinforcement Learning

The purpose of deep reinforcement learning (DRL) is to train an agent interacting with the environment to maximize its total rewards [163]. DRL can be regarded as learning via the Markov Decision Process, defined by the tuple $\{S, A, R, P\}$, where S is the set of states (environment condition), A is the set of actions (agent), R is the function mapping state-action pairs to rewards, and P is the transition probability (the probability of next state after performing actions on current state). The goal of DRL is to learn the policy π (a function mapping given state to an action) that maximizes the sum of discounted future rewards $J(\pi) = \mathbb{E}[\sum_i \gamma^i R(s_i, a_i)]$, where γ is the discount factor on the future reward (meaning rewards in more future are less important) [163]. In Deep Q-learning, the DNN models are utilized to learn the value functions (expected rewards for a state-action pair) for each action given the input state.

Due to the complex agent and environment conditions and limited training states, there also exist two types of uncertainty sources: data and model uncertainty. Data uncertainty can arise from the intrinsic randomness in the interactions between the agent and environment, which causes randomness in the reward R, the transition functions P, and the randomness in the next state value distribution. To characterize the data uncertainty arising from those sources, the distributional RL [11] takes a probabilistic perspective on learning the rewards functions instead of approximating the expectation of the value. Thus the approach can implement risk-aware behavior on the agent. A similar approach is proposed to quantify the data uncertainty in DRL aiming for curiosity-based learning in the face of unpredictable transitions [114]. The following work [32] extends the parametric distribution to non-parametric prediction interval methods to quantify the data uncertainty and avoid the explicit parametric format. The approach corresponds to the literature we discuss in section 5.1. On the other hand, given the limited training state space, there exists high model uncertainty. The DNN model may not learn the optimum policy function and miss the unexplored state spaces, which potentially give higher rewards. This means the DRL model faces a trade-off between exploitation and exploration. Exploration means utilizing what the model has learned and choosing the best policy to maximize future rewards. Exploration refers to choosing the unexplored state to learn more about possible high state-action pairs. The challenge of effective exploration is connected to model uncertainty. The higher model uncertainty means the model is not learned well in the given state and requires more exploration of that sample. For example, deep ensemble Q-network [28] is proposed to inject model uncertainty into Q learning for more efficient exploration sampling. To reduce the computational overhead, the Dropout Q-functions [68] method is proposed to use MC-dropout for model uncertainty quantification. The following work [132] demonstrates the previous ensemble and dropout methods may produce a poor approximation to the model uncertainty in cases where state density does not correlate with the true uncertainty. To overcome the shortcoming, they suggest adding a random prior to the ensemble DQNs.

In summary, both data and model uncertainty are crucial aspects of DRL for more efficient policy learning and exploration. Many works inspired by DNN uncertainty quantification have been proposed to improve the performance of DRL.

7 FUTURE DIRECTION

We identify some research gaps and list several future directions that current literature has not explored or has little coverage from both the methodologies and application perspectives.

7.1 Combine UQ with DNN explainability

The explanation for DNN model predictions has been increasingly crucial because it provides tools for understanding and diagnosing the model's prediction. Recently, many explainability methods, termed explainers [173], have been introduced in the category of local feature attribution methods. That is, methods that return a real-valued score for each feature of a given data sample, representing the feature's relative importance for the sample prediction. These explanations are local in that each data sample may have a different explanation. Using local feature attribution methods, therefore, helps users better understand nonlinear and complex black-box models. Both uncertainty quantification and explanation are important for a robust, trustworthy AI model. Current methodologies consider two directions separately, we consider it could enable a more trustworthy AI system if combining them. Though many methodologies have been proposed for more precise uncertainty quantification, very few techniques attempt to explain why uncertainty exists in the predictions.

There are two possible directions to combine the power of explanations and uncertainty quantification: First, existing explanation methods could be potentially improved after considering the prediction uncertainty since those uncertain samples' explanations may not be trustworthy and can be omitted [190, 193]. Second, from another perspective, after obtaining the uncertainty quantification, we can leverage the existing post hoc explanation methods to understand the reason that the model is uncertain [157]. For example, it is intriguing to ask the question of why the prediction is uncertain and which set of input features are uncertain, or due to which layer of the model is imperfect.

7.2 Structured Uncertainty Quantification

Structured data are samples that are interdependent with each other, violating the common i.i.d assumption [8**?**]. Examples are imaging data, spatiotemporal data, and graphs. Deep learning has been widely used to model structured data, but the uncertainty of its prediction is not often quantified. Here, we list future research directions for the three different types of structured data.

7.2.1 Imaging and inverse problem. The goal of the imaging process is to reconstruct an unknown image from measurements, which is an inverse problem commonly used in medical imaging (e.g., magnetic resonance imaging and X-ray computed tomography) and geophysical inversion (e.g., seismic inversion) [45, 47, 160]. However, this process is challenging due to the limited and noisy information used to determine the original image, leading to structured uncertainty and correlations between nearby pixels in the reconstructed image [82]. To overcome this issue, current research in uncertainty quantification of inverse problems employs conditional deep generative models, such as cVAE, cGAN, and conditional normalizing flow models [3, 40, 42]. These methods utilize a low-dimensional latent space for image generation but may overlook unique data characteristics, such as structural constraints from domain physics in certain types of image data, such as remote sensing images, MRI images, or geological subsurface images [75, 156, 160]. The use of physics-informed

models may improve uncertainty quantification in these cases. It's promising to incorporate the physics constraints for quantifying the uncertainty associated with the imaging process.

7.2.2 Spatiotemporal data. Spatiotemporal data are special due to the violation of the common assumption that samples follow an identical and independent distribution [71, 76, 155**?**]. Uncertainty quantification of spatiotemporal deep learning poses several unique challenges. First, the analysis of spatiotemporal data requires the co-registration of different maps (e.g., points, lines, polygons, geo-raster) into the same spatial reference system. The process is subject to registration uncertainty due to GPS errors or annotation mistakes in map generation [72, 73]. Such registration uncertainty causes troubles when training deep neural networks [61]. Second, implicit dependency structures exist in continuous space and time (e.g., spatial and temporal autocorrelation, and temporal dynamics). Thus, the uncertainty quantification process should be aware of such a dependency structure. Third, spatiotemporal non-stationary requires characterizing uncertainty due to out-of-distribution samples [71, 155]. In addition, a different level of uncertainty exists based on the nearby training sample density. Traditionally, the Gaussian process has been widely used to quantify spatial uncertainty. However, for deep neural network models, new techniques are needed that consider sample density both in the non-spatial feature space and in the geographic space.

7.2.3 Graph data. Graph data is a general type of structured data with nodes and edge connections. Graph neural networks (GNNs) have been widely used for graph applications related to node classification and edge (link) prediction. However, UQ for GNN models has been less explored. Some work utilizes existing UQ techniques for GNN models [46] without considering their unique characteristics. First, predictions on a graph are structured, so the UQ module needs to consider such structural dependency. Second, many GNN models assume a fixed graph topology from training and test instances (e.g., spectral-based methods [36]). Uncertainty exists in GNN predictions due to the shift of graph topology from training graphs and test graphs. Similarly, uncertainty exists when the graph is perturbed by removing nodes and edges. Finally, many real-world graph problems are spatiotemporal at the same time (e.g., traffic flow prediction on road networks). Thus, challenges related to UQ for spatiotemporal deep learning also apply to graphs.

7.3 UQ for physics-aware DNN models

Many scientific applications can be described with a physics principle, e.g., the conservation law for diffusion process in the form of a partial differential equation (PDE). Deep learning shows a great capability of extracting complex patterns from massive data in scientific discoveries. However, *black-box* deep neural networks do not incorporate the fundamental physics principle of the system [81]. To address the challenge, physics-informed neural networks (PINN) [80, 87, 97, 185] attempt to incorporate physical principles and domain knowledge into deep learning to make physically consistent predictions. For example, considering a spatiotemporal PDE in the form of

$$u_t(x,t) + \mathcal{N}_x u(x,t) = 0, x \in \mathcal{D}, t \in \mathcal{T} \tag{27}$$

where $u(x,t)$ is the interesting physical variables to be modeled, which can be parameterized with a neural network, i.e., $u(x,t) = f_\theta(x,t)$, x represents the spatial coordinate, t is the time coordinate and $\mathcal{N}_x$ is the nonlinear differential operator. The intuition of the PINN model is to build a neural network that explicitly encodes Eq. 27 as residual loss, i.e., $r_\theta(x,t) = \partial_t f_\theta(x,t) - \mathcal{N}_x f_\theta(x,t)$ to control the optimization space of the neural network [80]. Thus, the physical constraints can be incorporated into the model training process as a soft penalty.

For many physical systems, the underlying physical principle generating the samples may be non-deterministic or unknown. The system is inherently chaotic and stochastic. For example, in weather forecasting and climate prediction problems, the state of the system is sensitive to the

initial conditions, in which a small perturbation in the nonlinear system can result in a large difference in the later state (*a.k.a. butterfly effect*) [81]. Even with a deterministic initial condition, the unknown physics equation (e.g., PDE) that drives the system can be stochastic, which is described by a stochastic differential equation. Uncertainty quantification is of vital importance to improve the prediction's reliability, especially under distribution shifts. To summarize, the uncertainty of physical system modeling can come from the following source. First, the initial and boundary conditions of the physical system are non-deterministic, and the system may be chaotic [174]. Second, the inherent physical principle may not be perfectly known or the parameter of the governing equation may be stochastic, i.e., in an imperfect physical system, the conservation law of heat may be violated in a non-closed system [35, 185].

These cases indicate that for the stochastic physical system, there exists inherent *data uncertainty*. Thus, a natural way to model distributions and incorporate stochasticity and uncertainty into the neural network is through probabilistic models. Because of the unique characteristics of physical data, there exist several challenges for quantifying the uncertainty in PINN. First, the system requires considering the physical principle and its uncertainty simultaneously. The incorporation of physical constraints can significantly reduce the data and model uncertainty. Second, there are various sources of uncertainty, which may arise from the inherent physical system randomness, the measurement error, and the limited knowledge of the physical governing equation.

One direction of uncertainty quantification for PINN is to build a probabilistic neural network $p_\theta(\boldsymbol{u}|\boldsymbol{x}, t, \boldsymbol{z})$ for propagating uncertainty originating from various sources, where $\boldsymbol{u}(\boldsymbol{x}, t)$ represents the spatio-temporal random field with the explanatory spatial variable $\boldsymbol{x}$ and temporal variable t. $\boldsymbol{z}$ is a latent variable that follows a prior distribution $p(\boldsymbol{z})$ and aim to encode the variability of the high-dimensional observation $\boldsymbol{u}$ into low-dimensional embedding. Many approaches based on the deep generative model have been proposed to leverage their capability of probabilistic modeling for structured outputs [35, 51, 128].

7.4 UQ for Large Language Models

In recent years, large language models (LLMs) have demonstrated remarkable capabilities in generating coherent and contextually relevant text across various applications, from natural language processing to decision-making tasks. These models, such as OpenAI's GPT-4 [2], have shown proficiency in tasks ranging from text summarization and translation to more complex problem-solving and creative writing. However, despite their impressive performance, a critical challenge remains: how to ensure accurate uncertainty quantification to enhance the trustworthiness of these models? Existing research in LLMs uncertainty quantification mainly falls into two main categories: uncertainty estimation, and confidence calibration [53]. Uncertainty estimation methods for LLMs includes logit-based methods [43], model internal state-based methods [144], and consistency-based estimation [112]. Logit-based methods use the logits in the model output layer to compute the class entropy of output tokens. Internal state-based methods use the variability of sample embedding from model intermediate layers to quantify uncertainty. The embedding that is far from the majority of others indicates high uncertainty. Consistency-based methods measure the consistency between different model outputs from a sampling process and use the consistency as the uncertainty score [86, 99, 112]. For uncertainty estimation in LLMs, it is important to consider the semantic equivalence of the generated answers as different model outputs may look different in the generated tokens but similar in semantics. Graph-based [99] and semantic methods [89] propose alternative strategies for confidence estimation based on the semantic pattern, using a semantics similarity graph of different model outputs for uncertainty quantification. For confidence calibration, the goal is to adjust the model so that the quantified uncertainty from the above methods is aligned with prediction accuracy [103, 116]. However, the field is still in its infancy. In future research, more

work needs to be done to incorporate the natural ambiguity of language. For example, the same token sequences may have different semantic meanings in different contexts. As discussed in [53], benchmarking datasets and UQ methods for multi-modal foundation models are missing.

8 CONCLUSION

This paper presents a systematic survey on uncertainty quantification for DNNs based on their types of uncertainty sources. We categorize existing literature into three groups: model uncertainty, data uncertainty, and the combination of the two. In addition, we analyze the advantages and disadvantages of each approach corresponding to the subtype of uncertainty source it addresses. The uncertainty source and unique challenge of various applications in different domains and ML problems are also summarized. We list several future research directions.

REFERENCES

[1] Moloud Abdar, Farhad Pourpanah, Sadiq Hussain, Dana Rezazadegan, Li Liu, Mohammad Ghavamzadeh, Paul Fieguth, Xiaochun Cao, Abbas Khosravi, U Rajendra Acharya, et al. 2021. A review of uncertainty quantification in deep learning: Techniques, applications and challenges. *Information Fusion* 76 (2021), 243–297.

[2] Josh Achiam, Steven Adler, Sandhini Agarwal, Lama Ahmad, Ilge Akkaya, Florencia Leoni Aleman, Diogo Almeida, Janko Altenschmidt, Sam Altman, Shyamal Anadkat, et al. 2023. Gpt-4 technical report. *arXiv preprint arXiv:2303.08774* (2023).

[3] Jonas Adler and Ozan Öktem. 2018. Deep bayesian inversion. *arXiv preprint arXiv:1811.05910* (2018).

[4] Firoj Alam, Muhammad Imran, and Ferda Ofli. 2017. Image4act: Online social media image processing for disaster response. In *Proceedings of the 2017 IEEE/ACM international conference on advances in social networks analysis and mining 2017*. 601–604.

[5] Anastasios N Angelopoulos and Stephen Bates. 2021. A gentle introduction to conformal prediction and distribution-free uncertainty quantification. *arXiv preprint arXiv:2107.07511* (2021).

[6] Anastasios N Angelopoulos, Stephen Bates, et al. 2023. Conformal prediction: A gentle introduction. *Foundations and Trends® in Machine Learning* 16, 4 (2023), 494–591.

[7] Martin Arjovsky, Soumith Chintala, and Léon Bottou. 2017. Wasserstein generative adversarial networks. In *International conference on machine learning*. PMLR, 214–223.

[8] Gökhan BakIr, Thomas Hofmann, Alexander J Smola, Bernhard Schölkopf, and Ben Taskar. 2007. *Predicting structured data*. MIT press.

[9] Wentao Bao, Qi Yu, and Yu Kong. 2021. Evidential deep learning for open set action recognition. In *Proceedings of the IEEE/CVF International Conference on Computer Vision*. 13349–13358.

[10] Edmon Begoli, Tanmoy Bhattacharya, and Dimitri Kusnezov. 2019. The need for uncertainty quantification in machine-assisted medical decision making. *Nature Machine Intelligence* 1, 1 (2019), 20–23.

[11] Marc G Bellemare, Will Dabney, and Rémi Munos. 2017. A distributional perspective on reinforcement learning. In *International Conference on Machine Learning*. PMLR, 449–458.

[12] Yoshua Bengio, Aaron Courville, and Pascal Vincent. 2013. Representation learning: A review and new perspectives. *IEEE transactions on pattern analysis and machine intelligence* 35, 8 (2013), 1798–1828.

[13] Viktor Bengs, Eyke Hüllermeier, and Willem Waegeman. 2023. On second-order scoring rules for epistemic uncertainty quantification. In *International Conference on Machine Learning*. PMLR, 2078–2091.

[14] Christopher M Bishop. 1994. Mixture density networks. (1994).

[15] Jarosław Błasiok and Preetum Nakkiran. 2023. Smooth ECE: Principled reliability diagrams via kernel smoothing. *arXiv preprint arXiv:2309.12236* (2023).

[16] David M Blei, Alp Kucukelbir, and Jon D McAuliffe. 2017. Variational inference: A review for statisticians. *Journal of the American statistical Association* 112, 518 (2017), 859–877.

[17] James M Bower and Hamid Bolouri. 2001. *Computational modeling of genetic and biochemical networks*. MIT press.

[18] Eric Bradford, Artur M Schweidtmann, Dongda Zhang, Keju Jing, and Ehecatl Antonio del Rio-Chanona. 2018. Dynamic modeling and optimization of sustainable algal production with uncertainty using multivariate Gaussian processes. *Computers & Chemical Engineering* 118 (2018), 143–158.

[19] Glenn W Brier. 1950. Verification of forecasts expressed in terms of probability. *Monthly weather review* 78, 1 (1950), 1–3.

[20] Steven L Brunton and J Nathan Kutz. 2022. *Data-driven science and engineering: Machine learning, dynamical systems, and control*. Cambridge University Press.

[21] Jin Cao, Yanhui Jiang, Chang Yu, Feiwei Qin, and Zekun Jiang. 2024. Rough set improved therapy-based metaverse assisting system. *arXiv preprint arXiv:2406.04465* (2024).
[22] Michele Caprio, Souradeep Dutta, Kuk Jin Jang, Vivian Lin, Radoslav Ivanov, Oleg Sokolsky, and Insup Lee. 2023. Imprecise Bayesian neural networks. *arXiv preprint arXiv:2302.09656* (2023).
[23] Jie Chang, Zhonghao Lan, Changmao Cheng, and Yichen Wei. 2020. Data uncertainty learning in face recognition. In *Proceedings of the IEEE/CVF Conference on Computer Vision and Pattern Recognition*. 5710–5719.
[24] Bertrand Charpentier, Daniel Zügner, and Stephan Günnemann. 2020. Posterior network: Uncertainty estimation without ood samples via density-based pseudo-counts. *Advances in Neural Information Processing Systems* 33 (2020), 1356–1367.
[25] Haoxian Chen, Ziyi Huang, Henry Lam, Huajie Qian, and Haofeng Zhang. 2021. Learning prediction intervals for regression: Generalization and calibration. In *International Conference on Artificial Intelligence and Statistics*. PMLR, 820–828.
[26] Wei Chen and Mark Fuge. 2019. Synthesizing designs with interpart dependencies using hierarchical generative adversarial networks. *Journal of Mechanical Design* 141, 11 (2019), 111403.
[27] Xiang Chen, Andres Diaz-Pinto, Nishant Ravikumar, and Alejandro F Frangi. 2021. Deep learning in medical image registration. *Progress in Biomedical Engineering* 3, 1 (2021), 012003.
[28] Xinyue Chen, Che Wang, Zijian Zhou, and Keith Ross. 2021. Randomized ensembled double q-learning: Learning fast without a model. *arXiv preprint arXiv:2101.05982* (2021).
[29] Reynold Cheng, Tobias Emrich, Hans-Peter Kriegel, Nikos Mamoulis, Matthias Renz, Goce Trajcevski, and Andreas Züfle. 2014. Managing uncertainty in spatial and spatio-temporal data. In *2014 IEEE 30th International Conference on Data Engineering*. IEEE, 1302–1305.
[30] Jiwoong Choi, Dayoung Chun, Hyun Kim, and Hyuk-Jae Lee. 2019. Gaussian yolov3: An accurate and fast object detector using localization uncertainty for autonomous driving. In *Proceedings of the IEEE/CVF International Conference on Computer Vision*. 502–511.
[31] Dan C Cireşan, Alessandro Giusti, Luca M Gambardella, and Jürgen Schmidhuber. 2013. Mitosis detection in breast cancer histology images with deep neural networks. In *International conference on medical image computing and computer-assisted intervention*. Springer, 411–418.
[32] Will Dabney, Mark Rowland, Marc Bellemare, and Rémi Munos. 2018. Distributional reinforcement learning with quantile regression. In *Proceedings of the AAAI Conference on Artificial Intelligence*, Vol. 32.
[33] Andreas Damianou. 2015. *Deep Gaussian processes and variational propagation of uncertainty*. Ph. D. Dissertation. University of Sheffield.
[34] Andreas C Damianou, Michalis K Titsias, and Neil Lawrence. 2016. Variational inference for latent variables and uncertain inputs in Gaussian processes. (2016).
[35] Arka Daw, M Maruf, and Anuj Karpatne. 2021. PID-GAN: A GAN Framework based on a Physics-informed Discriminator for Uncertainty Quantification with Physics. In *Proceedings of the 27th ACM SIGKDD Conference on Knowledge Discovery & Data Mining*. 237–247.
[36] Michaël Defferrard, Xavier Bresson, and Pierre Vandergheynst. 2016. Convolutional neural networks on graphs with fast localized spectral filtering. *Advances in neural information processing systems* 29 (2016).
[37] Jia Deng, Wei Dong, Richard Socher, Li-Jia Li, Kai Li, and Li Fei-Fei. 2009. Imagenet: A large-scale hierarchical image database. In *2009 IEEE conference on computer vision and pattern recognition*. Ieee, 248–255.
[38] Tianchen Deng, Siyang Liu, Xuan Wang, Yejia Liu, Danwei Wang, and Weidong Chen. 2023. ProSGNeRF: Progressive Dynamic Neural Scene Graph with Frequency Modulated Auto-Encoder in Urban Scenes. *arXiv preprint arXiv:2312.09076* (2023).
[39] Tianchen Deng, Yanbo Wang, Hongle Xie, Hesheng Wang, Jingchuan Wang, Danwei Wang, and Weidong Chen. 2024. NeSLAM: Neural Implicit Mapping and Self-Supervised Feature Tracking With Depth Completion and Denoising. *arXiv preprint arXiv:2403.20034* (2024).
[40] Alexander Denker, Maximilian Schmidt, Johannes Leuschner, Peter Maass, and Jens Behrmann. 2020. Conditional normalizing flows for low-dose computed tomography image reconstruction. *arXiv preprint arXiv:2006.06270* (2020).
[41] Stefan Depeweg. 2019. *Modeling epistemic and aleatoric uncertainty with bayesian neural networks and latent variables*. Ph. D. Dissertation. Technische Universität München.
[42] Garoe Dorta, Sara Vicente, Lourdes Agapito, Neill DF Campbell, and Ivor Simpson. 2018. Structured uncertainty prediction networks. In *Proceedings of the IEEE Conference on Computer Vision and Pattern Recognition*. 5477–5485.
[43] Jinhao Duan, Hao Cheng, Shiqi Wang, Chenan Wang, Alex Zavalny, Renjing Xu, Bhavya Kailkhura, and Kaidi Xu. 2023. Shifting attention to relevance: Towards the uncertainty estimation of large language models. *arXiv preprint arXiv:2307.01379* (2023).
[44] Michael W Dusenberry, Dustin Tran, Edward Choi, Jonas Kemp, Jeremy Nixon, Ghassen Jerfel, Katherine Heller, and Andrew M Dai. 2020. Analyzing the role of model uncertainty for electronic health records. In *Proceedings of the*

ACM Conference on Health, Inference, and Learning. 204–213.
[45] Vineet Edupuganti, Morteza Mardani, Shreyas Vasanawala, and John Pauly. 2020. Uncertainty quantification in deep MRI reconstruction. *IEEE Transactions on Medical Imaging* 40, 1 (2020), 239–250.
[46] Boyuan Feng, Yuke Wang, and Yufei Ding. 2021. Uag: Uncertainty-aware attention graph neural network for defending adversarial attacks. In *Proceedings of the AAAI Conference on Artificial Intelligence*, Vol. 35. 7404–7412.
[47] Jeffrey A Fessler. 2010. Model-based image reconstruction for MRI. *IEEE signal processing magazine* 27, 4 (2010), 81–89.
[48] Fish Florida and Conservation Commission Wildlife. 2021. Florida Fish and Wildlife Conservation Commission Data. (2021). 10.5067/ORBVIEW-2/SEAWIFS/L2/OC/2018
[49] Karl Friston, Jérémie Mattout, Nelson Trujillo-Barreto, John Ashburner, and Will Penny. 2007. Variational free energy and the Laplace approximation. *Neuroimage* 34, 1 (2007), 220–234.
[50] Yarin Gal and Zoubin Ghahramani. 2016. Dropout as a bayesian approximation: Representing model uncertainty in deep learning. In *international conference on machine learning*. PMLR, 1050–1059.
[51] Yihang Gao and Michael K Ng. 2022. Wasserstein generative adversarial uncertainty quantification in physics-informed neural networks. *J. Comput. Phys.* 463 (2022), 111270.
[52] Jakob Gawlikowski, Cedrique Rovile Njieutcheu Tassi, Mohsin Ali, Jongseok Lee, Matthias Humt, Jianxiang Feng, Anna Kruspe, Rudolph Triebel, Peter Jung, Ribana Roscher, et al. 2021. A survey of uncertainty in deep neural networks. *arXiv preprint arXiv:2107.03342* (2021).
[53] Jiahui Geng, Fengyu Cai, Yuxia Wang, Heinz Koeppl, Preslav Nakov, and Iryna Gurevych. 2023. A survey of language model confidence estimation and calibration. *arXiv preprint arXiv:2311.08298* (2023).
[54] Biraja Ghoshal, Allan Tucker, Bal Sanghera, and Wai Lup Wong. 2021. Estimating uncertainty in deep learning for reporting confidence to clinicians in medical image segmentation and diseases detection. *Computational Intelligence* 37, 2 (2021), 701–734.
[55] Xuan Gong, Luckyson Khaidem, Wentao Zhu, Baochang Zhang, and David Doermann. 2022. Uncertainty learning towards unsupervised deformable medical image registration. In *Proceedings of the IEEE/CVF Winter Conference on Applications of Computer Vision*. 2484–2493.
[56] Ian Goodfellow, Jean Pouget-Abadie, Mehdi Mirza, Bing Xu, David Warde-Farley, Sherjil Ozair, Aaron Courville, and Yoshua Bengio. 2020. Generative adversarial networks. *Commun. ACM* 63, 11 (2020), 139–144.
[57] Alex Graves. 2011. Practical variational inference for neural networks. *Advances in neural information processing systems* 24 (2011).
[58] Axel Brando Guillaumes. 2017. *Mixture density networks for distribution and uncertainty estimation*. Ph. D. Dissertation. Universitat Politècnica de Catalunya. Facultat d'Informàtica de Barcelona.
[59] Chuan Guo, Geoff Pleiss, Yu Sun, and Kilian Q Weinberger. 2017. On calibration of modern neural networks. In *International conference on machine learning*. PMLR, 1321–1330.
[60] Reihaneh H Hariri, Erik M Fredericks, and Kate M Bowers. 2019. Uncertainty in big data analytics: survey, opportunities, and challenges. *Journal of Big Data* 6, 1 (2019), 1–16.
[61] Wenchong He, Zhe Jiang, Marcus Kriby, Yiqun Xie, Xiaowei Jia, Da Yan, and Yang Zhou. 2022. Quantifying and Reducing Registration Uncertainty of Spatial Vector Labels on Earth Imagery. In *Proceedings of the 28th ACM SIGKDD Conference on Knowledge Discovery and Data Mining*. 554–564.
[62] Yotam Hechtlinger, Barnabás Póczos, and Larry Wasserman. 2018. Cautious deep learning. *arXiv preprint arXiv:1805.09460* (2018).
[63] Alice Hein, Stefan Röhrl, Thea Grobel, Manuel Lengl, Nawal Hafez, Martin Knopp, Christian Klenk, Dominik Heim, Oliver Hayden, and Klaus Diepold. 2022. A Comparison of Uncertainty Quantification Methods for Active Learning in Image Classification. In *2022 International Joint Conference on Neural Networks (IJCNN)*. IEEE, 1–8.
[64] Dan Hendrycks and Kevin Gimpel. 2016. A baseline for detecting misclassified and out-of-distribution examples in neural networks. *arXiv preprint arXiv:1610.02136* (2016).
[65] Tomislav Hengl, Jorge Mendes de Jesus, Gerard BM Heuvelink, Maria Ruiperez Gonzalez, Milan Kilibarda, Aleksandar Blagotić, Wei Shangguan, Marvin N Wright, Xiaoyuan Geng, Bernhard Bauer-Marschallinger, et al. 2017. SoilGrids250m: Global gridded soil information based on machine learning. *PLoS one* 12, 2 (2017), e0169748.
[66] Brian Hie, Bryan D Bryson, and Bonnie Berger. 2020. Leveraging uncertainty in machine learning accelerates biological discovery and design. *Cell systems* 11, 5 (2020), 461–477.
[67] Geoffrey E Hinton and Drew Van Camp. 1993. Keeping the neural networks simple by minimizing the description length of the weights. In *Proceedings of the sixth annual conference on Computational learning theory*. 5–13.
[68] Takuya Hiraoka, Takahisa Imagawa, Taisei Hashimoto, Takashi Onishi, and Yoshimasa Tsuruoka. 2021. Dropout Q-Functions for Doubly Efficient Reinforcement Learning. *arXiv preprint arXiv:2110.02034* (2021).
[69] Eyke Hüllermeier and Willem Waegeman. 2021. Aleatoric and epistemic uncertainty in machine learning: An introduction to concepts and methods. *Machine Learning* 110, 3 (2021), 457–506.

[70] Xiaowei Jia, Jacob Zwart, Jeffrey Sadler, Alison Appling, Samantha Oliver, Steven Markstrom, Jared Willard, Shaoming Xu, Michael Steinbach, Jordan Read, et al. 2021. Physics-guided recurrent graph model for predicting flow and temperature in river networks. In *Proceedings of the 2021 SIAM International Conference on Data Mining (SDM)*. SIAM, 612–620.

[71] Zhe Jiang. 2018. A survey on spatial prediction methods. *IEEE Transactions on Knowledge and Data Engineering* 31, 9 (2018), 1645–1664.

[72] Zhe Jiang, Wenchong He, Marcus Kirby, Sultan Asiri, and Da Yan. 2021. Weakly Supervised Spatial Deep Learning based on Imperfect Vector Labels with Registration Errors. In *Proceedings of the 27th ACM SIGKDD Conference on Knowledge Discovery & Data Mining*. 767–775.

[73] Zhe Jiang, Wenchong He, Marcus Stephen Kirby, Arpan Man Sainju, Shaowen Wang, Lawrence V Stanislawski, Ethan J Shavers, and E Lynn Usery. 2022. Weakly Supervised Spatial Deep Learning for Earth Image Segmentation Based on Imperfect Polyline Labels. *ACM Transactions on Intelligent Systems and Technology (TIST)* 13, 2 (2022), 1–20.

[74] Zhe Jiang, Arpan Man Sainju, Yan Li, Shashi Shekhar, and Joseph Knight. 2019. Spatial ensemble learning for heterogeneous geographic data with class ambiguity. *ACM Transactions on Intelligent Systems and Technology (TIST)* 10, 4 (2019), 1–25.

[75] Zhe Jiang and Shashi Shekhar. 2017. Spatial big data science. *Schweiz: Springer International Publishing AG* (2017).

[76] Zhe Jiang, Liang Zhao, Xun Zhou, Robert N Stewart, Junbo Zhang, Shashi Shekhar, and Jieping Ye. 2022. DeepSpatial'22: The 3rd International Workshop on Deep Learning for Spatiotemporal Data, Applications, and Systems. In *Proceedings of the 28th ACM SIGKDD Conference on Knowledge Discovery and Data Mining*. 4878–4879.

[77] Laurent Valentin Jospin, Hamid Laga, Farid Boussaid, Wray Buntine, and Mohammed Bennamoun. 2022. Hands-on Bayesian neural networks—A tutorial for deep learning users. *IEEE Computational Intelligence Magazine* 17, 2 (2022), 29–48.

[78] AUDUN. JSANG. 2018. *Subjective Logic: A formalism for reasoning under uncertainty*. Springer.

[79] Hamed Karimi and Reza Samavi. 2023. Quantifying deep learning model uncertainty in conformal prediction. In *Proceedings of the AAAI Symposium Series*, Vol. 1. 142–148.

[80] George Em Karniadakis, Ioannis G Kevrekidis, Lu Lu, Paris Perdikaris, Sifan Wang, and Liu Yang. 2021. Physics-informed machine learning. *Nature Reviews Physics* 3, 6 (2021), 422–440.

[81] K Kashinath, M Mustafa, A Albert, JL Wu, C Jiang, S Esmaeilzadeh, K Azizzadenesheli, R Wang, A Chattopadhyay, A Singh, et al. 2021. Physics-informed machine learning: case studies for weather and climate modelling. *Philosophical Transactions of the Royal Society A* 379, 2194 (2021), 20200093.

[82] Alex Kendall and Yarin Gal. 2017. What uncertainties do we need in bayesian deep learning for computer vision? *Advances in neural information processing systems* 30 (2017).

[83] Sookyung Kim, Hyojin Kim, Joonseok Lee, Sangwoong Yoon, Samira Ebrahimi Kahou, Karthik Kashinath, and Mr Prabhat. 2019. Deep-hurricane-tracker: Tracking and forecasting extreme climate events. In *2019 IEEE Winter Conference on Applications of Computer Vision (WACV)*. IEEE, 1761–1769.

[84] Diederik P Kingma and Max Welling. 2013. Auto-encoding variational bayes. *arXiv preprint arXiv:1312.6114* (2013).

[85] Simon Kohl, Bernardino Romera-Paredes, Clemens Meyer, Jeffrey De Fauw, Joseph R Ledsam, Klaus Maier-Hein, SM Eslami, Danilo Jimenez Rezende, and Olaf Ronneberger. 2018. A probabilistic u-net for segmentation of ambiguous images. *Advances in neural information processing systems* 31 (2018).

[86] Maia Kotelanski, Robert Gallo, Ashwin Nayak, and Thomas Savage. 2023. Methods to Estimate Large Language Model Confidence. *arXiv preprint arXiv:2312.03733* (2023).

[87] Aditi Krishnapriyan, Amir Gholami, Shandian Zhe, Robert Kirby, and Michael W Mahoney. 2021. Characterizing possible failure modes in physics-informed neural networks. *Advances in Neural Information Processing Systems* 34 (2021), 26548–26560.

[88] Agustinus Kristiadi, Matthias Hein, and Philipp Hennig. 2021. Learnable uncertainty under laplace approximations. In *Uncertainty in Artificial Intelligence*. PMLR, 344–353.

[89] Lorenz Kuhn, Yarin Gal, and Sebastian Farquhar. 2023. Semantic uncertainty: Linguistic invariances for uncertainty estimation in natural language generation. *arXiv preprint arXiv:2302.09664* (2023).

[90] Balaji Lakshminarayanan, Alexander Pritzel, and Charles Blundell. 2017. Simple and scalable predictive uncertainty estimation using deep ensembles. *Advances in neural information processing systems* 30 (2017).

[91] Yann LeCun, Yoshua Bengio, and Geoffrey Hinton. 2015. Deep learning. *nature* 521, 7553 (2015), 436–444.

[92] Hong Joo Lee, Jung Uk Kim, Sangmin Lee, Hak Gu Kim, and Yong Man Ro. 2020. Structure boundary preserving segmentation for medical image with ambiguous boundary. In *Proceedings of the IEEE/CVF conference on computer vision and pattern recognition*. 4817–4826.

[93] Xian Yeow Lee, Aditya Balu, Daniel Stoecklein, Baskar Ganapathysubramanian, and Soumik Sarkar. 2019. A case study of deep reinforcement learning for engineering design: Application to microfluidic devices for flow sculpting. *Journal of Mechanical Design* 141, 11 (2019), 111401.

[94] Robert J Lempert, Steven W Popper, Carlos Calvo Hernandez, et al. 2022. *Transportation Planning for Uncertain Times: A Practical Guide to Decision Making Under Deep Uncertainty for MPOs*. Technical Report. United States. Federal Highway Administration.

[95] Junyi Li, Tianyi Tang, Wayne Xin Zhao, Jian-Yun Nie, and Ji-Rong Wen. 2021. Pre-trained Language Models for Text Generation: A Survey. *Comput. Surveys* (2021).

[96] Yiqun Li, Songjian Chai, Guibin Wang, Xian Zhang, and Jing Qiu. 2022. Quantifying the Uncertainty in Long-Term Traffic Prediction Based on PI-ConvLSTM Network. *IEEE Transactions on Intelligent Transportation Systems* 23, 11 (2022), 20429–20441.

[97] Zongyi Li, Nikola Kovachki, Kamyar Azizzadenesheli, Burigede Liu, Kaushik Bhattacharya, Andrew Stuart, and Anima Anandkumar. 2020. Fourier neural operator for parametric partial differential equations. *arXiv preprint arXiv:2010.08895* (2020).

[98] Richard J Licata and Piyush M Mehta. 2022. Uncertainty quantification techniques for data-driven space weather modeling: thermospheric density application. *Scientific Reports* 12, 1 (2022), 7256.

[99] Zhen Lin, Shubhendu Trivedi, and Jimeng Sun. 2023. Generating with confidence: Uncertainty quantification for black-box large language models. *arXiv preprint arXiv:2305.19187* (2023).

[100] Dehao Liu and Yan Wang. 2019. Multi-fidelity physics-constrained neural network and its application in materials modeling. *Journal of Mechanical Design* 141, 12 (2019), 121403.

[101] Jeremiah Liu, Zi Lin, Shreyas Padhy, Dustin Tran, Tania Bedrax Weiss, and Balaji Lakshminarayanan. 2020. Simple and principled uncertainty estimation with deterministic deep learning via distance awareness. *Advances in Neural Information Processing Systems* 33 (2020), 7498–7512.

[102] Jeremiah Zhe Liu, Shreyas Padhy, Jie Ren, Zi Lin, Yeming Wen, Ghassen Jerfel, Zachary Nado, Jasper Snoek, Dustin Tran, and Balaji Lakshminarayanan. 2022. A simple approach to improve single-model deep uncertainty via distance-awareness. *Journal of Machine Learning Research* 23 (2022), 1–63.

[103] Linyu Liu, Yu Pan, Xiaocheng Li, and Guanting Chen. 2024. Uncertainty Estimation and Quantification for LLMs: A Simple Supervised Approach. *arXiv preprint arXiv:2404.15993* (2024).

[104] Rui Liu, Xuanzhen Xu, Yuwei Shen, Armando Zhu, Chang Yu, Tianjian Chen, and Ye Zhang. 2024. Enhanced detection classification via clustering svm for various robot collaboration task. *arXiv preprint arXiv:2405.03026* (2024).

[105] Tyler J Loftus, Benjamin Shickel, Matthew M Ruppert, Jeremy A Balch, Tezcan Ozrazgat-Baslanti, Patrick J Tighe, Philip A Efron, William R Hogan, Parisa Rashidi, Gilbert R Upchurch Jr, et al. 2022. Uncertainty-aware deep learning in healthcare: a scoping review. *PLOS digital health* 1, 8 (2022), e0000085.

[106] Christos Louizos and Max Welling. 2017. Multiplicative normalizing flows for variational bayesian neural networks. In *International Conference on Machine Learning*. PMLR, 2218–2227.

[107] Charles Lu, Andréanne Lemay, Ken Chang, Katharina Höbel, and Jayashree Kalpathy-Cramer. 2022. Fair conformal predictors for applications in medical imaging. In *Proceedings of the AAAI Conference on Artificial Intelligence*, Vol. 36. 12008–12016.

[108] David JC MacKay. 1992. A practical Bayesian framework for backpropagation networks. *Neural computation* 4, 3 (1992), 448–472.

[109] Andrey Malinin and Mark Gales. 2018. Predictive uncertainty estimation via prior networks. *Advances in neural information processing systems* 31 (2018).

[110] Tanwi Mallick, Prasanna Balaprakash, and Jane Macfarlane. 2022. Deep-Ensemble-Based Uncertainty Quantification in Spatiotemporal Graph Neural Networks for Traffic Forecasting. *arXiv preprint arXiv:2204.01618* (2022).

[111] Potsawee Manakul, Adian Liusie, and Mark Gales. 2023. SelfCheckGPT: Zero-Resource Black-Box Hallucination Detection for Generative Large Language Models. In *Proceedings of the 2023 Conference on Empirical Methods in Natural Language Processing*, Houda Bouamor, Juan Pino, and Kalika Bali (Eds.). Association for Computational Linguistics, Singapore, 9004–9017. https://doi.org/10.18653/v1/2023.emnlp-main.557

[112] Potsawee Manakul, Adian Liusie, and Mark JF Gales. 2023. Selfcheckgpt: Zero-resource black-box hallucination detection for generative large language models. *arXiv preprint arXiv:2303.08896* (2023).

[113] Christos Markos, JQ James, and Richard Yi Da Xu. 2021. Capturing uncertainty in unsupervised GPS trajectory segmentation using Bayesian deep learning. In *Proceedings of the AAAI Conference on Artificial Intelligence*, Vol. 35. 390–398.

[114] Augustine Mavor-Parker, Kimberly Young, Caswell Barry, and Lewis Griffin. 2022. How to stay curious while avoiding noisy tvs using aleatoric uncertainty estimation. In *International Conference on Machine Learning*. PMLR, 15220–15240.

[115] José Mena, Oriol Pujol, and Jordi Vitrià. 2021. A survey on uncertainty estimation in deep learning classification systems from a bayesian perspective. *ACM Computing Surveys (CSUR)* 54, 9 (2021), 1–35.

[116] Sabrina J Mielke, Arthur Szlam, Emily Dinan, and Y-Lan Boureau. 2022. Reducing conversational agents' over-confidence through linguistic calibration. *Transactions of the Association for Computational Linguistics* 10 (2022), 857–872.

[117] Aaron Mishkin, Frederik Kunstner, Didrik Nielsen, Mark Schmidt, and Mohammad Emtiyaz Khan. 2018. Slang: Fast structured covariance approximations for bayesian deep learning with natural gradient. *Advances in Neural Information Processing Systems* 31 (2018).
[118] Zhaobin Mo and Yongjie Fu. 2022. TrafficFlowGAN: Physics-informed Flow based Generative Adversarial Network for Uncertainty Quantification. In *European Conference on Machine Learning and Data Mining (ECML PKDD)*.
[119] Max Mowbray, Thomas Savage, Chufan Wu, Ziqi Song, Bovinille Anye Cho, Ehecatl A Del Rio-Chanona, and Dongda Zhang. 2021. Machine learning for biochemical engineering: A review. *Biochemical Engineering Journal* 172 (2021), 108054.
[120] Kevin P Murphy. 2012. *Machine learning: a probabilistic perspective*. MIT press.
[121] Mahdi Pakdaman Naeini, Gregory Cooper, and Milos Hauskrecht. 2015. Obtaining well calibrated probabilities using bayesian binning. In *Proceedings of the AAAI conference on artificial intelligence*, Vol. 29.
[122] Space Flight Center NASA Goddard. 2019. Sea-viewing Wide Field-of-view Sensor (SeaWiFS) Ocean Color Data. (2019). https://doi.org/10.5067/ORBVIEW-2/SEAWIFS/L2/OC/2018
[123] Parth Natekar, Avinash Kori, and Ganapathy Krishnamurthi. 2020. Demystifying brain tumor segmentation networks: interpretability and uncertainty analysis. *Frontiers in computational neuroscience* 14 (2020), 6.
[124] Radford M Neal. 2012. *Bayesian learning for neural networks*. Vol. 118. Springer Science & Business Media.
[125] Andre T Nguyen, Fred Lu, Gary Lopez Munoz, Edward Raff, Charles Nicholas, and James Holt. 2022. Out of Distribution Data Detection Using Dropout Bayesian Neural Networks. *arXiv preprint arXiv:2202.08985* (2022).
[126] Vu-Linh Nguyen, Mohammad Hossein Shaker, and Eyke Hüllermeier. 2022. How to measure uncertainty in uncertainty sampling for active learning. *Machine Learning* 111, 1 (2022), 89–122.
[127] Jeremy Nixon, Michael W Dusenberry, Linchuan Zhang, Ghassen Jerfel, and Dustin Tran. 2019. Measuring Calibration in Deep Learning.. In *CVPR workshops*, Vol. 2.
[128] Philipp Oberdiek, Gernot A Fink, and Matthias Rottmann. 2022. UQGAN: A Unified Model for Uncertainty Quantification of Deep Classifiers trained via Conditional GANs. *arXiv preprint arXiv:2201.13279* (2022).
[129] Philip Odonkor and Kemper Lewis. 2019. Data-driven design of control strategies for distributed energy systems. *Journal of Mechanical Design* 141, 11 (2019), 111404.
[130] Sangeun Oh, Yongsu Jung, Seongsin Kim, Ikjin Lee, and Namwoo Kang. 2019. Deep generative design: Integration of topology optimization and generative models. *Journal of Mechanical Design* 141, 11 (2019), 111405.
[131] Shu Lih Oh, Yuki Hagiwara, U Raghavendra, Rajamanickam Yuvaraj, N Arunkumar, M Murugappan, and U Rajendra Acharya. 2020. A deep learning approach for Parkinson's disease diagnosis from EEG signals. *Neural Computing and Applications* 32, 15 (2020), 10927–10933.
[132] Ian Osband, John Aslanides, and Albin Cassirer. 2018. Randomized prior functions for deep reinforcement learning. *Advances in Neural Information Processing Systems* 31 (2018).
[133] Yaniv Ovadia, Emily Fertig, Jie Ren, Zachary Nado, David Sculley, Sebastian Nowozin, Joshua Dillon, Balaji Lakshminarayanan, and Jasper Snoek. 2019. Can you trust your model's uncertainty? evaluating predictive uncertainty under dataset shift. *Advances in neural information processing systems* 32 (2019).
[134] Mohit Pandey, Michael Fernandez, Francesco Gentile, Olexandr Isayev, Alexander Tropsha, Abraham C Stern, and Artem Cherkasov. 2022. The transformational role of GPU computing and deep learning in drug discovery. *Nature Machine Intelligence* 4, 3 (2022), 211–221.
[135] Yutian Pang, Xinyu Zhao, Hao Yan, and Yongming Liu. 2021. Data-driven trajectory prediction with weather uncertainties: A Bayesian deep learning approach. *Transportation Research Part C: Emerging Technologies* 130 (2021), 103326.
[136] Tim Pearce, Alexandra Brintrup, Mohamed Zaki, and Andy Neely. 2018. High-quality prediction intervals for deep learning: A distribution-free, ensembled approach. In *International conference on machine learning*. PMLR, 4075–4084.
[137] Dieter Pfoser and Christian S Jensen. 1999. Capturing the uncertainty of moving-object representations. In *International Symposium on Spatial Databases*. Springer, 111–131.
[138] Konstantin Posch and Juergen Pilz. 2020. Correlated parameters to accurately measure uncertainty in deep neural networks. *IEEE Transactions on Neural Networks and Learning Systems* 32, 3 (2020), 1037–1051.
[139] Konstantin Posch, Jan Steinbrener, and Jürgen Pilz. 2019. Variational inference to measure model uncertainty in deep neural networks. *arXiv preprint arXiv:1902.10189* (2019).
[140] Sergey Prokudin, Peter Gehler, and Sebastian Nowozin. 2018. Deep directional statistics: Pose estimation with uncertainty quantification. In *Proceedings of the European conference on computer vision (ECCV)*. 534–551.
[141] Yu Qin, Zhiwen Liu, Chenghao Liu, Yuxing Li, Xiangzhu Zeng, and Chuyang Ye. 2021. Super-Resolved q-Space deep learning with uncertainty quantification. *Medical Image Analysis* 67 (2021), 101885.
[142] Anant Raj and Francis Bach. 2022. Convergence of uncertainty sampling for active learning. In *International Conference on Machine Learning*. PMLR, 18310–18331.

[143] Markus Reichstein, Gustau Camps-Valls, Bjorn Stevens, Martin Jung, Joachim Denzler, and Nuno Carvalhais. 2019. Deep learning and process understanding for data-driven Earth system science. *Nature* 566, 7743 (2019), 195–204.
[144] Jie Ren, Jiaming Luo, Yao Zhao, Kundan Krishna, Mohammad Saleh, Balaji Lakshminarayanan, and Peter J Liu. 2022. Out-of-distribution detection and selective generation for conditional language models. In *The Eleventh International Conference on Learning Representations*.
[145] Pengzhen Ren, Yun Xiao, Xiaojun Chang, Po-Yao Huang, Zhihui Li, Brij B Gupta, Xiaojiang Chen, and Xin Wang. 2021. A survey of deep active learning. *ACM computing surveys (CSUR)* 54, 9 (2021), 1–40.
[146] Hippolyt Ritter, Aleksandar Botev, and David Barber. 2018. Online structured laplace approximations for overcoming catastrophic forgetting. In *Proceedings of the 32nd International Conference on Neural Information Processing Systems*. 3742–3752.
[147] Hippolyt Ritter, Aleksandar Botev, and David Barber. 2018. A scalable laplace approximation for neural networks. In *6th International Conference on Learning Representations, ICLR 2018-Conference Track Proceedings*, Vol. 6. International Conference on Representation Learning.
[148] Hippolyt Ritter, Martin Kukla, Cheng Zhang, and Yingzhen Li. 2021. Sparse Uncertainty Representation in Deep Learning with Inducing Weights. *Advances in Neural Information Processing Systems* 34 (2021), 6515–6528.
[149] Nir Rosenfeld, Yishay Mansour, and Elad Yom-Tov. 2018. Discriminative learning of prediction intervals. In *International Conference on Artificial Intelligence and Statistics*. PMLR, 347–355.
[150] Tárik S Salem, Helge Langseth, and Heri Ramampiaro. 2020. Prediction intervals: Split normal mixture from quality-driven deep ensembles. In *Conference on Uncertainty in Artificial Intelligence*. PMLR, 1179–1187.
[151] Tim Salimans, Diederik Kingma, and Max Welling. 2015. Markov chain monte carlo and variational inference: Bridging the gap. In *International conference on machine learning*. PMLR, 1218–1226.
[152] Murat Sensoy, Lance Kaplan, and Melih Kandemir. 2018. Evidential deep learning to quantify classification uncertainty. *Advances in neural information processing systems* 31 (2018).
[153] Sina Shafaei, Stefan Kugele, Mohd Hafeez Osman, and Alois Knoll. 2018. Uncertainty in machine learning: A safety perspective on autonomous driving. In *Computer Safety, Reliability, and Security: SAFECOMP 2018 Workshops, ASSURE, DECSoS, SASSUR, STRIVE, and WAISE, Västerås, Sweden, September 18, 2018, Proceedings 37*. Springer, 458–464.
[154] Glenn Shafer and Vladimir Vovk. 2008. A tutorial on conformal prediction. *Journal of Machine Learning Research* 9, 3 (2008).
[155] Shashi Shekhar, Zhe Jiang, Reem Y Ali, Emre Eftelioglu, Xun Tang, Venkata MV Gunturi, and Xun Zhou. 2015. Spatiotemporal data mining: A computational perspective. *ISPRS International Journal of Geo-Information* 4, 4 (2015), 2306–2338.
[156] Shu-Fu Shih, Sevgi Gokce Kafali, Kara L Calkins, and Holden H Wu. 2022. Uncertainty-aware physics-driven deep learning network for free-breathing liver fat and R2* quantification using self-gated stack-of-radial MRI. *Magnetic Resonance in Medicine* (2022).
[157] Dylan Slack, Anna Hilgard, Sameer Singh, and Himabindu Lakkaraju. 2021. Reliable post hoc explanations: Modeling uncertainty in explainability. *Advances in neural information processing systems* 34 (2021), 9391–9404.
[158] Edward Snelson and Zoubin Ghahramani. 2005. Sparse Gaussian processes using pseudo-inputs. *Advances in neural information processing systems* 18 (2005).
[159] Kihyuk Sohn, Honglak Lee, and Xinchen Yan. 2015. Learning structured output representation using deep conditional generative models. *Advances in neural information processing systems* 28 (2015).
[160] Jian Sun, Kristopher A Innanen, and Chao Huang. 2021. Physics-guided deep learning for seismic inversion with hybrid training and uncertainty analysis. *Geophysics* 86, 3 (2021), R303–R317.
[161] Shengyang Sun, Changyou Chen, and Lawrence Carin. 2017. Learning structured weight uncertainty in bayesian neural networks. In *Artificial Intelligence and Statistics*. PMLR, 1283–1292.
[162] Dedy Suryadi and Harrison M Kim. 2019. A data-driven methodology to construct customer choice sets using online data and customer reviews. *Journal of Mechanical Design* 141, 11 (2019), 111103.
[163] Richard S Sutton and Andrew G Barto. 2018. *Reinforcement learning: An introduction*. MIT press.
[164] Jakub Swiatkowski, Kevin Roth, Bastiaan Veeling, Linh Tran, Joshua Dillon, Jasper Snoek, Stephan Mandt, Tim Salimans, Rodolphe Jenatton, and Sebastian Nowozin. 2020. The k-tied normal distribution: A compact parameterization of Gaussian mean field posteriors in Bayesian neural networks. In *International Conference on Machine Learning*. PMLR, 9289–9299.
[165] Sunil Thulasidasan, Gopinath Chennupati, Jeff A Bilmes, Tanmoy Bhattacharya, and Sarah Michalak. 2019. On mixup training: Improved calibration and predictive uncertainty for deep neural networks. *Advances in Neural Information Processing Systems* 32 (2019).
[166] Michalis Titsias. 2009. Variational learning of inducing variables in sparse Gaussian processes. In *Artificial intelligence and statistics*. PMLR, 567–574.

[167] Trung Q Trinh, Markus Heinonen, Luigi Acerbi, and Samuel Kaski. 2022. Tackling covariate shift with node-based Bayesian neural networks. In *International Conference on Machine Learning*. PMLR, 21751–21775.
[168] Ivan Ustyuzhaninov, Ieva Kazlauskaite, Markus Kaiser, Erik Bodin, Neill Campbell, and Carl Henrik Ek. 2020. Compositional uncertainty in deep Gaussian processes. In *Conference on Uncertainty in Artificial Intelligence*. PMLR, 480–489.
[169] Joost van Amersfoort, Lewis Smith, Andrew Jesson, Oscar Key, and Yarin Gal. 2021. On Feature Collapse and Deep Kernel Learning for Single Forward Pass Uncertainty. *arXiv preprint arXiv:2102.11409* (2021).
[170] Joost Van Amersfoort, Lewis Smith, Yee Whye Teh, and Yarin Gal. 2020. Uncertainty estimation using a single deep deterministic neural network. In *International conference on machine learning*. PMLR, 9690–9700.
[171] Gijs Van Tulder and Marleen De Bruijne. 2016. Combining generative and discriminative representation learning for lung CT analysis with convolutional restricted Boltzmann machines. *IEEE transactions on medical imaging* 35, 5 (2016), 1262–1272.
[172] Aladin Virmaux and Kevin Scaman. 2018. Lipschitz regularity of deep neural networks: analysis and efficient estimation. *Advances in Neural Information Processing Systems* 31 (2018).
[173] Minh Vu and My T Thai. 2020. Pgm-explainer: Probabilistic graphical model explanations for graph neural networks. *Advances in neural information processing systems* 33 (2020), 12225–12235.
[174] Bin Wang, Jie Lu, Zheng Yan, Huaishao Luo, Tianrui Li, Yu Zheng, and Guangquan Zhang. 2019. Deep uncertainty quantification: A machine learning approach for weather forecasting. In *Proceedings of the 25th ACM SIGKDD International Conference on Knowledge Discovery & Data Mining*. 2087–2095.
[175] Jian Wang, Wei Deng, and Yuntao Guo. 2014. New Bayesian combination method for short-term traffic flow forecasting. *Transportation Research Part C: Emerging Technologies* 43 (2014), 79–94.
[176] Pengyue Wang, Yan Li, Shashi Shekhar, and William F Northrop. 2019. Uncertainty estimation with distributional reinforcement learning for applications in intelligent transportation systems: A case study. In *2019 IEEE Intelligent Transportation Systems Conference (ITSC)*. IEEE, 3822–3827.
[177] Florian Wenzel, Jasper Snoek, Dustin Tran, and Rodolphe Jenatton. 2020. Hyperparameter ensembles for robustness and uncertainty quantification. *Advances in Neural Information Processing Systems* 33 (2020), 6514–6527.
[178] Christopher KI Williams and Carl Edward Rasmussen. 2006. *Gaussian processes for machine learning*. Vol. 2. MIT press Cambridge, MA.
[179] Andrew Wilson and Hannes Nickisch. 2015. Kernel interpolation for scalable structured Gaussian processes (KISS-GP). In *International conference on machine learning*. PMLR, 1775–1784.
[180] Andrew Gordon Wilson, Zhiting Hu, Ruslan Salakhutdinov, and Eric P Xing. 2016. Deep kernel learning. In *Artificial intelligence and statistics*. PMLR, 370–378.
[181] Christopher Wolf, Maximilian Karl, and Patrick van der Smagt. 2016. Variational inference with hamiltonian monte carlo. *arXiv preprint arXiv:1609.08203* (2016).
[182] Dongxia Wu, Liyao Gao, Matteo Chinazzi, Xinyue Xiong, Alessandro Vespignani, Yi-An Ma, and Rose Yu. 2021. Quantifying Uncertainty in Deep Spatiotemporal Forecasting. In *Proceedings of the 27th ACM SIGKDD Conference on Knowledge Discovery & Data Mining*. 1841–1851.
[183] Ziwei Xu, Sanjay Jain, and Mohan Kankanhalli. 2024. Hallucination is inevitable: An innate limitation of large language models. *arXiv preprint arXiv:2401.11817* (2024).
[184] Chu-I Yang and Yi-Pei Li. 2023. Explainable uncertainty quantifications for deep learning-based molecular property prediction. *Journal of Cheminformatics* 15, 1 (2023), 13.
[185] Yibo Yang and Paris Perdikaris. 2019. Adversarial uncertainty quantification in physics-informed neural networks. *J. Comput. Phys.* 394 (2019), 136–152.
[186] Gal Yarin. 2016. Uncertainty in deep learning. *University of Cambridge, Cambridge* (2016).
[187] Jiaxuan You, Xiaocheng Li, Melvin Low, David Lobell, and Stefano Ermon. 2017. Deep gaussian process for crop yield prediction based on remote sensing data. In *Thirty-First AAAI conference on artificial intelligence*.
[188] Sheheryar Zaidi, Arber Zela, Thomas Elsken, Chris C Holmes, Frank Hutter, and Yee Teh. 2021. Neural ensemble search for uncertainty estimation and dataset shift. *Advances in Neural Information Processing Systems* 34 (2021), 7898–7911.
[189] Guodong Zhang, Shengyang Sun, David Duvenaud, and Roger Grosse. 2018. Noisy natural gradient as variational inference. In *International Conference on Machine Learning*. PMLR, 5852–5861.
[190] Xiaoge Zhang, Felix TS Chan, and Sankaran Mahadevan. 2022. Explainable machine learning in image classification models: An uncertainty quantification perspective. *Knowledge-Based Systems* 243 (2022), 108418.
[191] Xianli Zhang, Buyue Qian, Shilei Cao, Yang Li, Hang Chen, Yefeng Zheng, and Ian Davidson. 2020. INPREM: An interpretable and trustworthy predictive model for healthcare. In *Proceedings of the 26th ACM SIGKDD International Conference on Knowledge Discovery & Data Mining*. 450–460.

[192] Ling Zhao, Yujiao Song, Chao Zhang, Yu Liu, Pu Wang, Tao Lin, Min Deng, and Haifeng Li. 2019. T-gcn: A temporal graph convolutional network for traffic prediction. *IEEE Transactions on Intelligent Transportation Systems* 21, 9 (2019), 3848–3858.

[193] Xingyu Zhao, Wei Huang, Xiaowei Huang, Valentin Robu, and David Flynn. 2021. Baylime: Bayesian local interpretable model-agnostic explanations. In *Uncertainty in artificial intelligence*. PMLR, 887–896.

[194] Weitao Zhou, Zhong Cao, Yunkang Xu, Nanshan Deng, Xiaoyu Liu, Kun Jiang, and Diange Yang. 2022. Long-Tail Prediction Uncertainty Aware Trajectory Planning for Self-driving Vehicles. In *2022 IEEE 25th International Conference on Intelligent Transportation Systems (ITSC)*. IEEE, 1275–1282.

[195] Yuanshao Zhu, Yongchao Ye, Yi Liu, and JQ James. 2022. Cross-area travel time uncertainty estimation from trajectory data: a federated learning approach. *IEEE Transactions on Intelligent Transportation Systems* 23, 12 (2022), 24966–24978.